I.P.N. - 91406 ORSAY CEDEX

institut de physique nucléaire CNRS - IN2P3 UNIVERSITÉ PARIS - SUD

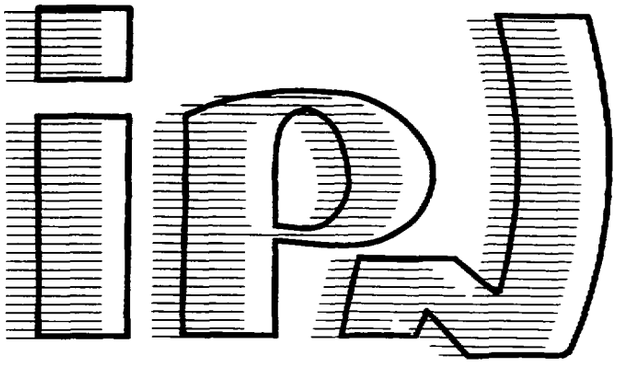

IPNO-DRE 93-11

GAS FILLED DETECTORS

Claude STEPHAN

**To be published in Handbook of Nuclear Decay Modes,
edited by D. N. Poenaru and W. Greiner,
CRC Press, Boca Raton, Florida.**

IPNO-DRE 93-11

GAS FILLED DETECTORS

Claude STEPHAN

To be published in Handbook of Nuclear Decay Modes,
edited by D. N. Poenaru and W. Greiner,
CRC Press, Boca Raton, Florida.

GAS FILLED DETECTORS

Claude STEPHAN

INSTITUT DE PHYSIQUE NUCLEAIRE
CNRS-IN2P3 Université Paris-Sud ORSAY, FRANCE

I. INTRODUCTION

Gas detectors are among the oldest and widespread types of instruments used in nuclear physics. They have found a regain of interest in the early 1970's with the acceleration of heavy ions which introduced new requirements: thin entrance windows, low pressure of operation, detectors set in vacuum, and chiefly the ability to work at the same time with particles with very different values of atomic number. They are radiation insensitive and they can compete advantageously with scintillators or solid state detectors which present pulse height defects increasing with Z, shortened life time due to large energy losses in the detector, small active areas. Gas detectors are extremely versatile: they can handle high counting rates and be used for energy measurements, position determination or for timing with all types of charged particles, and even with γ and X rays. They can easily fit every experimental condition and be built at a relatively low price although in large dimensions with the advantage to eventually be repaired on site during an experiment. Their disadvantages are essentially a relatively limited energy resolution and the necessity of a gas filling which might eventually mean leak or window problems. The main types of gas detectors, ionization chambers, proportional counters, and avalanche counters, which have become routine tools, will be described. Complex designs and new devices are also advocated. For a better understanding of their operating way, a resumé on the processes involved in such detectors is given.

II. BASIC PROCESSES INVOLVED

The processes involved in gas detectors have been extensively studied and are now well understood. A charged particle traversing a gaseous medium interacts essentially with it by Coulomb interactions. The electromagnetic field of the particle will produce excitation and ionization when interacting with the outer electrons of the atoms of the gas. The energy loss results of these discrete interactions between the projectile and atoms from the medium. These primary collisions then create electron-positive ion pairs which again will be able to interact with the medium. The characteristics of the signals from the different types of gas counters are strongly related to the created number of primary pairs. In the absence of other effects, ionic charges will rapidly loose their energy by multiple collisions with gas molecules while electrons will diffuse in the medium.

A. Energy Loss in Gas

Many review articles have been written on the subject of charged particle energy loss in matter.[1-2]

1. Light particle energy loss

The energy loss of particles depends on the energy transferred to electron of gas molecules during the interaction. The quantitative evaluation of the energy loss dT per length unit dX has been described a long time ago by Bethe and Bloch in the framework of relativistic quantum mechanics by the formula:

$$\frac{dT}{dX} = \frac{4\pi e^4 z^2}{m_0 V^2} nZ \left[ln\frac{2m_0 V^2}{I} - ln(1-\beta^2) - \beta^2 - \frac{C_K}{Z} \right] \quad (1)$$

where Z is the atomic number of the medium, I is its effective ionization potential which can be taken with a good approximation as $I = I_0 Z$, where $I_0 = 12$ eV; n is the number of interactions per volume unit, m_0 and e are the electron mass and charge, V and z are the velocity and charge state of projectile, $\beta = V/c$. C_K represents inner shell corrections and can usually be neglected.

In this equation (1) the projectile energy loss is a function of its velocity and not of its energy. The stopping power is then the product of two factors, one is a monotonically decreasing function of the velocity of the projectile, the second (between braces) increases logarithmically with it. This second term is responsible for the relativistic rise of the stopping power. If the energy is expressed in MeV and the thickness of the medium in gcm^{-2} one finds

$$\frac{4\pi e^4 z^2 nZ}{m_0 V^2} = 0.307\beta^{-2} z^2 \rho \frac{Z}{A} \quad MeV/gcm^{-2} \quad (2)$$

A, ρ, are respectively the mass and density of the medium. For molecular gases or mixtures, one takes average values for A, Z, and I in the Bethe formula.

2. Heavy ion energy loss

The Bethe formula (1) predicts with a good precision proton and alpha particle energy losses. Presently gas detectors are mostly used in nuclear physics for heavy ions. In order to apply the formula to these particles it is necessary to know the charge state z of the projectile. Indeed it depends on the energy of the ion and on the traversed medium. It means that z will even vary during its path in the gas when decelerating. This renders in most cases the formula (1) almost unusable for heavy ions. As stopping powers and ranges play an important role in many aspects of heavy-ion physics, semi empirical tables of energy loss of heavy ions have then been established by means of a scaling law based on a compilation of hundreds of experimental data.[3-5] The most recent tables by Hubert et al.[5] have used the following parameterization equations where alpha particles are chosen as reference projectiles.

$$S_{ion} = S_{He}\frac{(\gamma_{1,2}Z_1)^2_{ion}}{(\gamma_1 Z_1)^2_{He}} \tag{3}$$

with

$$\gamma_{1,2} = \gamma_1 f(Z_1, Z_2) \tag{4}$$

$$\gamma_1 = 1 - A(Z_1)exp\frac{-0.88V}{V_0 Z_1^{0.65}} \tag{5}$$

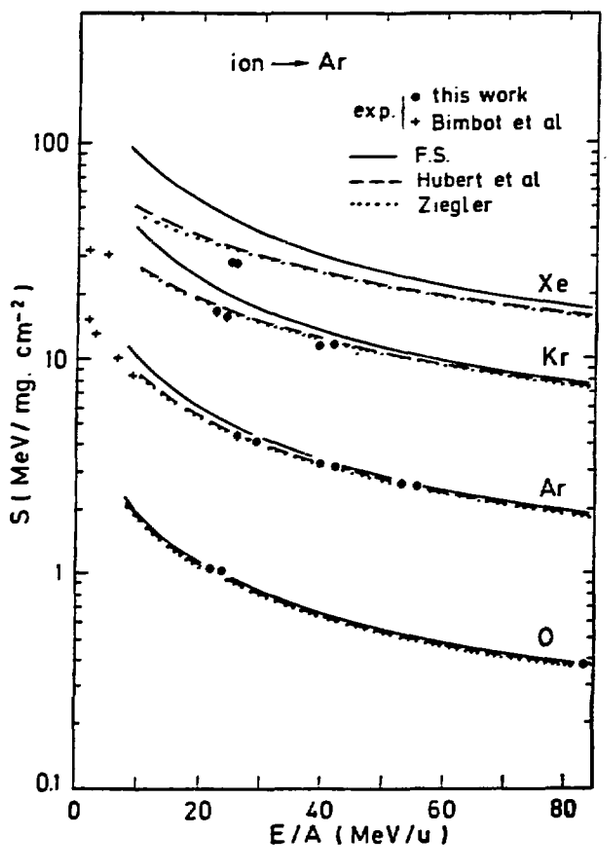

Figure 1. *Variation of the stopping power of Argon for O, Ar, Kr and Xe ions versus incident energy. The experimental points (full dots) are compared with calculated curves from Ziegler (dotted lines)*[4]*, from fully stripped approximation (solid lines) and from an effective charge parameterization valid for solid media (broken line)*[5]*. From Herault et al.*[7]

2.5 MeV/u and 500 MeV/u in a large sampling of solids. For gases, the authors find their tabulation valuable when the ions are fully stripped, but the energy loss of gases is decreased by 20% for ions which have a broad charge state distribution. This effect was first observed by Geissel et al.[6] in 1983. Figure 1 shows such differences obtained by Herault et al.[7] for the energy loss of Xe ions in argon. The authors interpret the difference by a density effect in solids.

3. Photon interactions

Gas detectors can also be used to detect gamma and X rays. Three major types of interaction mechanisms lead to the partial or complete transfer of the photon energy to electron energy: photoelectric absorption, Compton scattering and pair production as described in chapter X. In contrast with charged particles which loose gradually their energy, here these processes result in sudden energy deposit in the gas. The choice of the gas filling will then be determined essentially by its absorption capability, in order to get a high detection efficiency.

B. The relation between energy deposited and charge collection

1. Number of ion pairs created

Regardless of the detailed mechanisms involved, the practical quantity of interest is the total number of ion pairs created along the track of the radiation. The minimum energy I_0 which can be transferred for each interaction is between 10 and 20 eV, corresponding to the ejection of the least tightly bound electrons. However, other mechanisms like atom excitation which happen in distant collisions can lead to an energy loss of the incoming particle without removal of an electron from the gas molecule. Therefore, the average energy W which corresponds to an ion pair creation is substantially greater than the ionization energy. The parameter W does not depend much on the particle, its energy or even the nature of the gas. This feature is illustrated in table 1 where values of W for alpha particles, 340 MeV protons and β rays are given.[1,8]

From table 1 one can deduce that a 10 MeV particle will create about 3.10^5 ion pairs. There are fluctuations on the number of these ion pairs and these fluctuations can have important consequences on the energy resolution of the detector. It is necessary to distinguish two cases: when the particle deposits a large amount of energy in the detector or when it leaves in it only a small part of its total energy. In the first case, many gas detectors show an inherent fluctuation which is less than predicted by Poisson law. It simply means that when an important part of the energy of the particle is lost in the gas, there is a correlation between the number of collisions experienced by the particle and the energy lost at average in each collision.The Fano factor is introduced as an empirical constant by which the variance so found has to be multiplied to give the experimental value.[1]

In the other case, the ion pair fluctuations can conduct to serious limitations for thin low pressure detectors in which there are very few primary ionization events following Poisson-like statistics. As there are large fluctuations in the energy loss per impact, measured energy losses are broader than expected by a statistical variance only.[9] The energy loss distributions are characterized by an asymmetry with an excess of large energy losses as predicted by Landau and Vavilov.[10-11]. The relative probability of different processes induced by 31.5 MeV protons in a proportional counter are represented in figure 2.

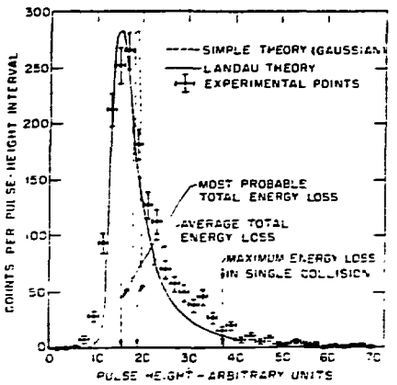

Figure 2. *Frequency distribution of energy losses of 31.5 MeV protons traversing proportional counter filled with 96% Ar and 4% CO_2. The histogram of experimental points is compared to the theoretical Landau distribution and a gaussian distribution based on ion-electron pair statistics. From Igo et al.*[12]

TABLE 1

Effective ionization potential $I_0(eV)$ and values of W(eV/ion pair) in various gases for α, β rays and 340 MeV protons. From FANO,[1] *and from SAULI,*[8] *where references are given.*

gases	I_0	W		
		α rays	β rays	340 MeV protons
He	24.6	42.7	42.3	
Ne	21.6	36.8	36.6	
Ar	15.8	26.4	26.4	
Kr	14.0	24.1	24.2	
Xe	12.1	21.9	22.0	
H_2	15.4	36.3	36.3	36.5
N_2	15.5	36.4	34.9	34.7
O_2	12.2	32.5	30.9	32.6
CO_2	13.7	34.0	32.9	
CH_4	13.1	29.0	27.3	
C_4H_{10}	10.8			23

2. Ion Drift

In gas detectors an electric field is applied across the gas volume inducing motion of ions and electrons along the field direction, named the drift velocity w. It results in a slow movement linearly proportional to the electric field E and inversely proportional to the gas pressure P. Table 2 gives experimental mobilities of several ions in different gases where the mobility μ is defined by the formula

$$w = \mu \frac{E}{P} \tag{6}$$

TABLE 2

Experimental mobilities of several ions in different gases, at normal conditions.[13]

Gas	Ions	Mobility $(cm^2V^{-1}sec{-}1)$
Ar	$(OCH_3)_2CH_2^+$	1.51
$isoC_4H_{10}$	$(OCH_3)_2CH_2^+$	0.55
$(OCH_3)_2CH_2$	$(OCH_3)_2CH_2^+$	0.26
Ar	$isoC_4H_{10}^+$	1.56
$isoC_4H_{10}$	$isoC_4H_{10}^+$	0.61
Ar	CH_4^+	1.87
CH_4	CH_4^+	2.26
Ar	CO_2^+	1.72
CO_2	CO_2^+	1.09

3. electron drift

The maximum energy T_M of electrons results from a collision between the projectile and an electron from the medium following a two body kinematics. Ejected electrons have a statistical energy distribution of the form

$$f(\lambda) = \frac{1}{\sqrt{2\pi}} e^{-\frac{1}{2}(\lambda + e^{-\lambda})} \tag{7}$$

In this formula due to Landau,[10] λ represents the normalized deviation from the most probable energy loss. These electrons, named δ electrons at the time of nuclear emulsions, are emitted at an angle given by a free electron approximation $cos^2\theta = \frac{T}{T_M}$. They will then drift in the gas volume. Due to their small size, the collisions with molecules of the medium are much less probable than for ions. Therefore these electrons move much faster in gas than ions by a factor 1000. Typical collection times in detectors are of the order of microseconds as compared to milliseconds for ions. In a formulation due to Townsend,[14] the drift velocity w can be written

$$w = \frac{e}{2m} E\tau \tag{8}$$

where τ is the mean time between collisions. The electron-atom cross sections vary with energy, due to complex quantum effects between the free electron and the electron shells of gas molecules. It means that τ will depend strongly on the electric field E and consequently the shape of the electron energy distribution is also E dependent. As an example, the drift velocity w of electrons through the gas of an ionization chamber, is about 5.10^6 cm/s.

Multiple collisions undergone by electrons during the drift outcome as a diffusion in the gas. Following the kinetic theory of gases, the proportion of electrons $\frac{dN}{N}$ found in the element dx, at the distance x from the origin after a time t , is given by a Gaussian distribution-like formula

$$\frac{dN}{N} = \frac{1}{\sqrt{4\pi Dt}} e^{x^2/4Dt} dx \tag{9}$$

where D is the diffusion coefficient; changes in the electron energy distribution due to the presence of an electric field result in a diffusion coefficient D dependent on the electric field E. This diffusion will result in a collection on a wider surface which will affect the position resolution. A small diffusion coefficient leads to a better position resolution

4. Recombination

Some of the many collisions of free electrons with gas atoms during the drift may result in charge neutralization. Recombination probability depends on charge carrier density and gas pressure. This process is of importance since the original charge is lost and will not contribute to the collected ionization signal. It can even happen that the free electron is collected by a neutral atom, creating a negative ion.

Collisions between ions and neutral atoms of gas have still a much higher probability to happen due to their very small mean free path. Charge transfer is possible either with a molecule of its own gas or with molecules with lower ionization potential. In gas mixtures, this process is very effective and rapidly removes all ions except the ones with the lower ionization potential. Negative ions may recombine with positive ions resulting in neutral atoms. In worse case these negative ions contribute to reduce the collected signal with their opposite charge.

5. The multiplication phenomenon

When a high electric field is applied on an electrode, the primary electrons acquire an energy larger than the ionization potential of the gas atoms. Thus, they can induce secondary ionizations and thc new free electrons can in turn be accelerated and produce further ionizations, generating a small avalanche. The development of such an avalanche and its quenching depends on the intensity of the electric field and on the nature of the gas filling. The gas mixture will be chosen in order to fulfill the experimental requirements, high gain, high counting rate, fast recovery, between others. More details are given in section IV devoted to proportional counters.

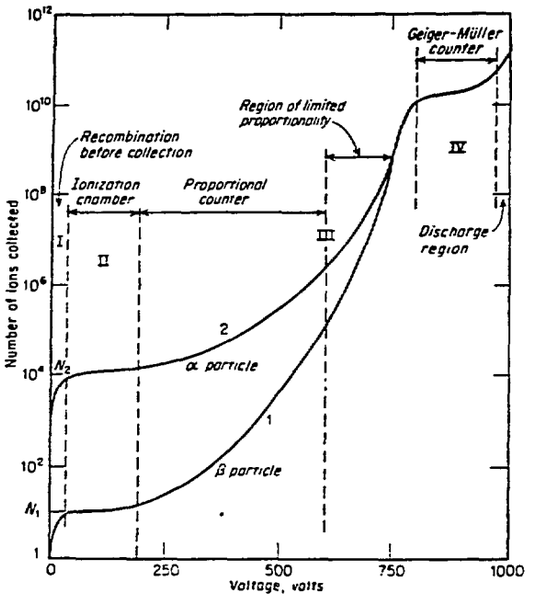

Figure 3. *The different regions of operation of gas filled detectors. The pulse amplitude is plotted for particles depositing a different amount of energy within the gas.*[15]

6. Different regions of operation of gas counters.

The collected charge is connected to the applied voltage difference between anode and cathode. Figure 3 after the Montgomerys in 1941 illustrates the different operating modes following the value of this voltage difference.[15] At very low voltage, recombination plays an important role. When the voltage is increased, full collection can be reached and the detector is said to be operating in the ionization chamber mode. If the electric field is still increased, near the anode surface a multiplication process begins and gains up to 10^4 are reached. The detector is said to be working in the proportional regime since the collected signal is still proportional to the deposited charge. If the voltage is increased again, the proportionality is gradually lost. Finally a saturated gain is reached in Geiger-Müller counters, or in certain conditions a new regime called the self quenching mode is obtained.

In the next sections the different types of detectors following these various modes will be described and recent applications will be presented.

III. IONIZATION CHAMBERS

Ionization chambers have been described by many authors.[16–18] They have been in operation for a very long time and in their principle there were no significant changes since the beginning. This type of detector has regained interest since 1975 with the development of heavy ion nuclear physics due to the very high stopping power of heavy ions. Consequently hardly feasible thin and homogeneous solid detectors (scintillators and silicon detectors mainly) can be advantageously replaced by gas chambers which in addition are radiation insensitive. Electronic linear amplification improvements have made their use competitive.

A. Principle of operation

The most simple type of chamber will consist in two electrodes made of two parallel plates maintaining a static electric field in between. In such chambers it is assumed that the applied electric field is sufficient to eliminate recombination effects and that negative charges are only due to free electrons. The constant electric field intensity E is given by the relation

$$E = \frac{V}{d} \tag{10}$$

where V is the voltage applied across the chamber electrodes distant by d. The situation is sketched in figure 4.

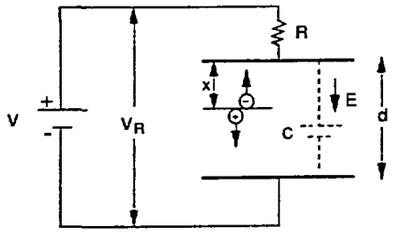

Figure 4. *Diagram of parallel plate ionization chamber. Parameters d and x are shown.*

We assume that a particle has produced n_0 ion pairs at a distance x from the anode. After a time t_e given by the electron drift, all the electrons have reached the anode. During the same time the ions moved very little but induced a charge on the anode. The signal voltage through a resistor denoted V_R will then be

$$V_R = \frac{n_0 e}{C}\frac{x}{d} \tag{11}$$

here C is the ionization chamber capacitance. By waiting long enough so that all ions be collected on the cathode, the maximum expected signal is

$$V_{max} = \frac{n_0 e}{C} \tag{12}$$

As these collection times are of milliseconds, for high counting rates, it is interesting to choose a much shorter collection time constant so that the collected pulse reflects only the electron drift. The output pulse as a function of time is represented in figure 5.

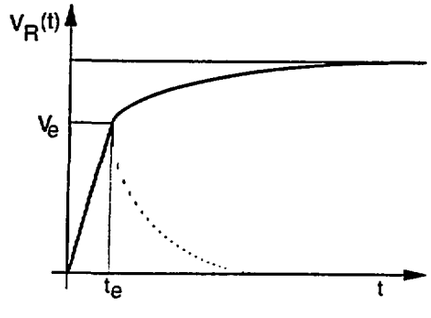

Figure 5. *Output pulse V_R as a function of collection time. The fast rise time corresponds to electron collection, the broken line represents the shape of output pulse with a time constant $RC \ll$ ion full time collection.*

Unfortunately, the collected signal V_R depends on the position x of the pair creations. To get rid of this dependence, Frisch has designed ionization chambers with a screening grid.

1. The gridded ionization chamber

The dependence of the pulse amplitude on the position of the ion pair creation can be removed with a chamber equipped with a "Frisch" grid. In this chamber the electrons have to traverse a grid set between the interaction volume and the anode. This grid is as transparent as possible, compatible with a good shielding efficiency. The grid is kept at an intermediate potential. Thus the pulse amplitudes obtained from collected electrons are not changed by the image charge of ions. An extensive study of grid effects by Buneman, Cranshaw and Harvey allows to evaluate the shielding efficiency of a Frisch grid.[19]

$$\sigma = \frac{p}{p + (\frac{s}{2\pi})(\frac{\rho^2}{4} - log\rho)} \quad \text{where} \quad \rho = \frac{2\pi a}{s} \tag{13}$$

In this formula, σ evaluates to which extent the grid will shield the collector anode from the electric field in the ionization chamber; p is the distance grid-anode, s is the wire interval, and a is the wire radius. For example, a Frisch grid made of wires 50 μm in diameter, 1 mm apart, distant from the anode by 1 cm and from the cathode by 5 cm, will give $\sigma = 0.971$. This value is very much satisfactory, since the grid has still a 95% mechanical transparency. Further, collection of electrons by the grid can be substantially avoided if the electric field set between grid and anode is somewhat larger than the ionization chamber electric field. All lines of electric field by-pass the grid under the condition (14) derived by Buneman et al.[19]

$$\frac{V_P - V_G}{V_G - V_A} \geq \frac{p + \rho p + 2\sigma\rho p}{d - \rho d - 2\sigma\rho p} \tag{14}$$

In this condition valuable for efficient shielding (σ should be close to 1) V_A, V_G, V_P are, respectively, the potentials applied to anode, grid and cathode; d is the distance grid-cathode.

2. Wall and window effects

The metallic walls of the chamber at a potential V = 0 distort the lines of force of the electric field, and consequently a fraction of the electrons are not collected. If walls are made of isolating material the situation is still worse since their potential can change with position and time, due to electrostatic charging up. This problem has been solved a long time ago with a guard ring surrounding the collector electrode on all sides. This name comes from the days when most often the ionization chambers were cylindrical, with a radioactive source deposited on one of the electrodes. Nowadays, usually the detected particle is emitted by an irradiated target from outside a parallelepipedic chamber. The particle reaches the ionizing volume through a window made of a thin plastic film.

Guard rings on the edges reduce the size of the effective volume. In front of the entrance window, they create a dead section where the energy of the particle is not measured. A clever solution consists to constitute an electric shielding with wires or aluminum strips evaporated on a plastic foil at a potential which varies linearly between the potentials of both electrodes. The efficiency of the shielding is a function of the distance between strips. A reasonable evaluation is to consider that electric field inhomogeneities disappear at a distance five times larger than the distance between strips.[20]

3. Observed signals

These detectors are mostly used in nuclear physics to detect heavy ions, to measure their total energy E, but also their energy loss ΔE in a small part of their total range, in order to determine their atomic number Z. As compared to solid state detectors, no pulse height defect on the heavy ion mass can be observed.[21] Indeed, the energy loss in a given medium thickness is a function of Z^c with $c \sim 2$. For this purpose, the anode is split in two or more parts to be able to identify in Z and measure the energy of all the heavy ions of interest.[22] In addition the gas pressure can also be adjusted.

A schematic drawing of a typical chamber is represented in figure 6, showing the different electrodes, the electric shielding and typical voltage values.[23]

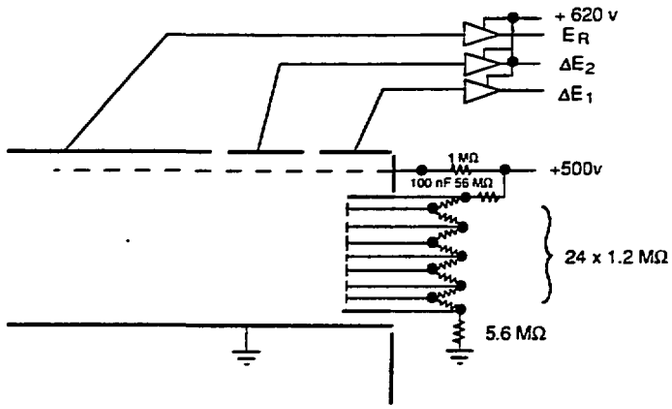

Figure 6. *Schematic drawing of a parallel plate ionization chamber, showing the splitting of anode in 3 parts and the potential distribution on the entrance window. The given voltages are for a 5 cm wide ionization space filled with isobutane at a pressure of 0.2 atmosphere.*[23]

Signals on the anodes due to electron collection must be amplified. The contribution of the electronic noise to the resolution is small in most cases, (10^{-4} of the collected signal typically). The actual resolution of the energy measurement is then given essentially by the fluctuations in the number of collected electrons and by energy straggling. For the

total residual energy left in the detector, a resolution better than 1% is always obtained and resolutions of 0.3 % can be achieved. In the evaluation of the total energy loss in the ionization chamber one must be aware that the entrance window is not usually flat due the gas pressure inside the chamber and vacuum outside.[24] As a result the residual energy left in the chamber will vary with the position height and should be taken into account.

Energy loss resolutions may not be as good for heavy ions as they use to be for light particles. This fact is connected with the charge state distribution of the projectile during its path through the medium. The charge state of the particle is determined by the competition between various atomic collisions processes, essentially electron capture, ionization, which cross sections depend on the relative velocities of the projectile and the bounded electron involved.[25] When velocities are similar, the projectile may undergo a few charge state changes during its trajectory inside the gas. Each time the stopping power will be modified. It means that each particle might have a different energy loss in a given gas volume. This is not true for the full range since all the energy of the particle is measured whatever the succession of involved processes, but is important when gases are used to identify the atomic number of the particle by energy loss determination. As a consequence of atomic processes involved, energy loss resolution in a detector will improve when the energy of the heavy ion increases but get worse with large Z values.

Much better energy loss resolutions are obtained with relativistic heavy ions. Ions are then most of the time fully stripped so that the effect mentioned above coming from charge state changes, is insignificant. Further, experimental results show a still better resolution than predicted by the collision theory presented in section II.A.2. Pfützner et al.[26] have measured

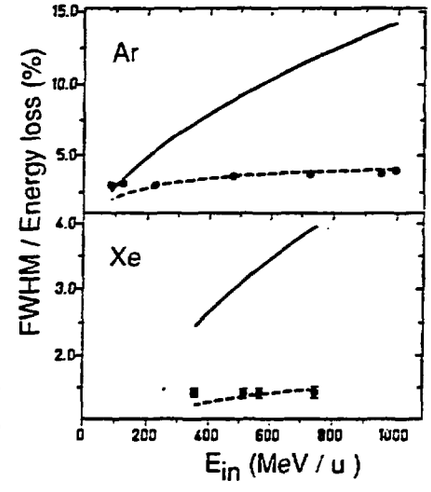

Figure 7. *Measured relative straggling of the energy deposition of Ar and Xe ions (dots), compared to standard collision theory (solid line) and to Badhwar theory (broken line). From Pfüzner et al.*[26]

energy deposition spectra using ^{40}Ar,^{86}Kr,^{136}Xe,^{197}Au ions with energies between 100 and 950 MeV/u. They obtain a very narrow energy loss distribution, Gaussian in shape, in

place of a Vavilov-Landau shape. The deviations from the standard collision theory can be understood by taking into account the high energy δ electrons which escape from the active volume. These energetic electrons contribute very little to the energy loss but participate to the energy straggling. Figure 7 shows the experimental results, a comparison with the standard theory and with a theory due to Badhwar taking into account the escape of δ electrons.[27]

B. Various designs of ionization chambers

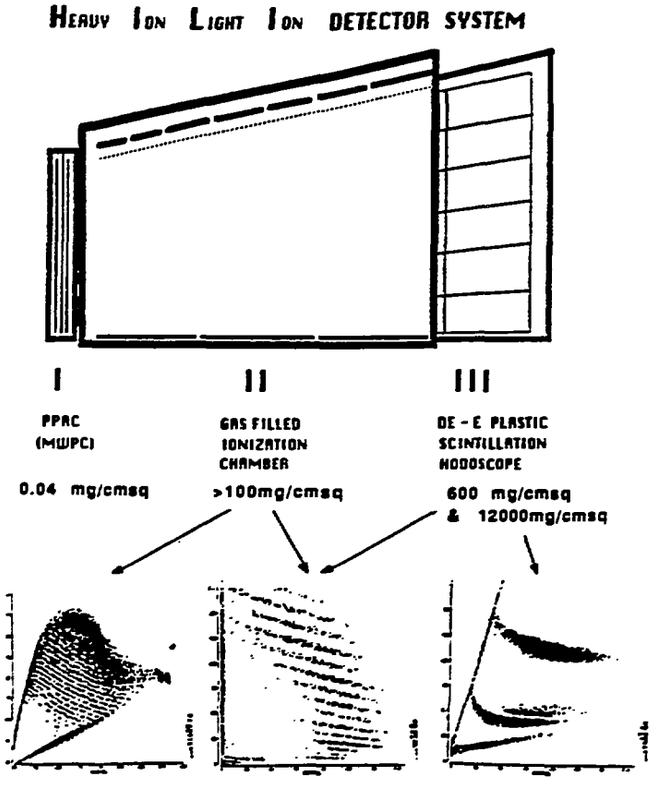

Figure 8. *A side view of the HILI detector showing the different layers and two-dimensional plots obtained by correlations between different layers used to identify various reaction products for the reaction* $^{79}Br + Al$.[28]

Since the renewal of ionization chambers due to the development of heavy ion physics, many detectors have been built in large dimensions, exceeding 100 cm deepness. Most of the time they are associated with other types of detectors in order to obtain a complete

identification of all reaction products in Z, A, energy and angle of emission, as shown in figure 8.[28]

1. Transmission chambers.

Figure 6 represents a classical ionization chamber in which the particle flux is parallel to the electrodes. Another design consists to build chambers in which the particle traverses the detector perpendicular to the electrodes. Such chambers have been used as first detectors of telescopes in which they serve for Z identification only. Very thin ΔE detectors for heavy ion experiments can be realized using thin entrance windows and low pressure filling gases. As the particle is not stopped in active volume of the chamber, the ion pairs are created all along the chamber crossing. The signal they induce on electrodes is then not position dependent, making unnecessary the use of a Frisch grid.

An example is given in figure 9 which represents a section of backward transmission ionization chambers of the INDRA set-up. This 4π detector is designed to identify any ion from Z = 1 up to 20 and to measure their energy above 1 MeV/u threshold.

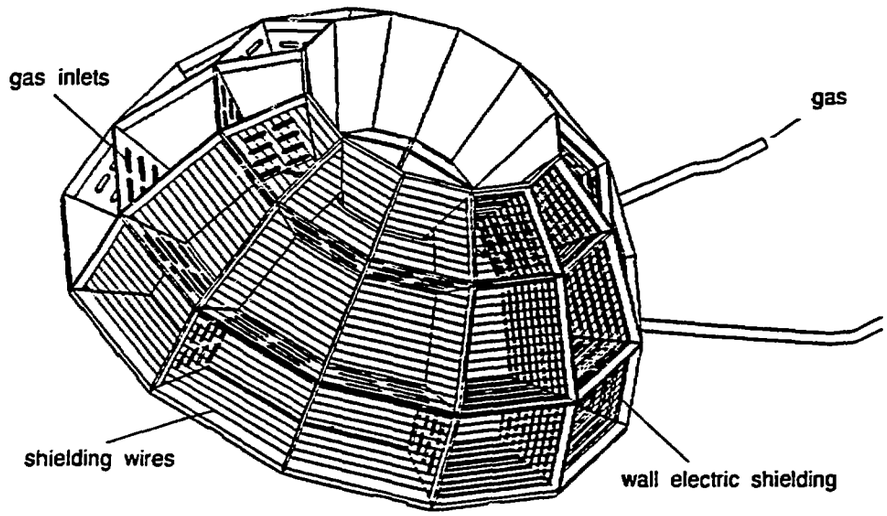

Figure 9. *Backward transmission ionization chambers of the 4π detector INDRA. With courtesy of part of the INDRA collaboration (GANIL Caen and DAPNIA-CEA Saclay).*

It has been realized by means of three member telescopes: a transmission ionization chamber, a transmission silicon detector and an iodine cesium crystal. Dead zones on the edges have been reduced to 2mm between telescopes. Each cell of the ionization chamber is only 5 cm wide, consequently the particle is never very far from the walls. The signal induced by the ion pairs is then shared between these walls and electrodes. To avoid a few per cent

error on the measured energy loss from this effect, a loose shielding grid made of thin wires every 5 mm has been added in front of the anode.

2. Position sensitive ionization chambers.

The most recent ionization chambers have been designed for heavy ion detection mainly. They were built in large dimensions, either because they must cover the total focal plane of a magnetic spectrometer, either time of flight determination is needed simultaneously and then the detector is set at a distance of the order of one meter from the target. Additional requirements have been introduced: angle of entrance in the detector, perpendicular position y, the possibility to accept more than one particle per event. Sann et al.[29] have built a conventional ionization chamber, but with a further grid half-way between the Frisch grid and the anode. This extra grid is made of wires oriented following equidistant radii from the target, separated by one degree. The electrons drifting through the grid induce a charge signal on the closer wires, giving the angle of entrance. The position in the perpendicular direction is obtained by the drift time of electrons from their origin to the Frisch grid. Another way to determine the position is to equip an ionization chamber with a stripped cathode like the detector designed for the mass separator LOHENGRIN at Grenoble.[30] In this detector, the cathode consists of an etched printed circuit board where copper strips, parallel to the beam, of 5 mm width alternate with isolators of 2 mm width.

A further development consists in an internal sectorization of the detector, to allow an improved counting rate capability and multiple event detection.[31] MUSIC (multiple sampling ionization chamber) detectors are in use, at GSI, Darmstadt,[32] associated with magnetic analysis like FRS and ALADIN.

3. Bragg chambers.

In order to identify heavy ions in a large range of atomic numbers and energies, it would be necessary to split the anode in as many electrodes as needed. To prevent this, Gruhn et al.[33] have proposed a new type of detector called Bragg chamber. The stopping power of a particle varies with the energy lost in the medium and becomes maximum at the end of its range. The position of this maximum called Bragg peak depends on the particle atomic number and its incident energy. Authors have built an ionization chamber like the transmission chambers described above but in which the heavy ions are stopped.[33–36] The charges collected on the anode are analysed in time, allowing the determination of the Bragg peak. On the other end, the integral of all collected charges gives the total energy of the ion. These informations are obtained either by digitalizing the signals, either by splitting the analogic signal in two parts with different time constants. It is important to choose a filling gas with a fast drift velocity in order to prevent recombinations and allow a reasonable counting rate. Gramegna et al.[37] have realized such a device which at 20 000 counts per

second still give $\frac{\Delta E}{E} = 0.9\%$ and $\frac{\Delta Z}{Z} = 50$ for 5 MeV/u ^{32}S incident beam.

An alternate solution consists to use a classical chamber with a transverse electric field equipped with a resistive anode allowing to determine the center of gravity of the Bragg peak with enough precision. A better solution has been adopted by Mittig et al.[38] for a 70 cm deep ionization chamber in which the resistive anode is replaced by 2 mm wide conducting strips connected to a delay line. A time measurement allows to know at which strip the ion has stopped. The total energy is obtained by summing the signals collected on the grid and the cathode. This device has been able to easily separate 30 MeV/u heavy ions up to Xenon as can be seen in the two-dimensional plot of figure 10.

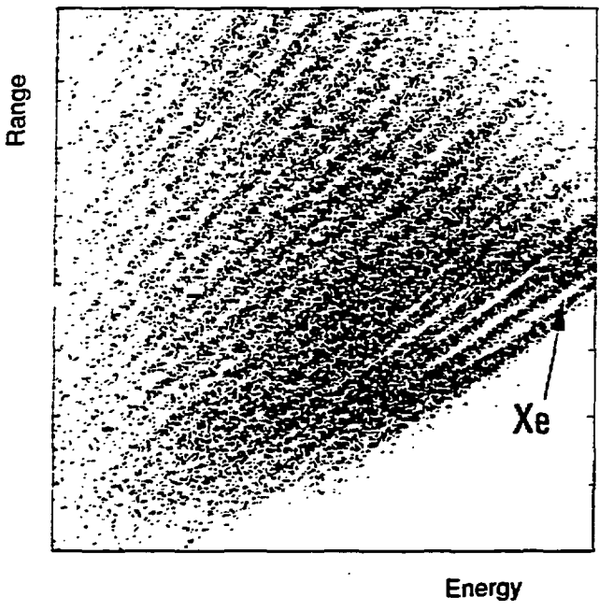

Figure 10. *Two dimensional plot of heavy ion ranges as a function of energy in Mittig et al detector.*[38] *All ions up to Xe can be identified.*

4. Direct current ionization chambers

Ionization chambers have been widely used for radiation dose measurements, i.e. gamma-ray exposure, radiation calibration, and accelerated beam monitoring. In direct current mode, it is possible to collect either free electrons, either negative charges, (see section IV.B for more details). Therefore any gas can fulfill this purpose, including those with high electron attachment probability. It is then very convenient to use air at atmospheric pressure as filling gas, if a denser gas is not absolutely needed. The ionization current can be measured with an electrometer by sensing the voltage drop through a series resistance of at least $10^9\Omega$ placed between the two electrodes. For a more stable amplification of the signal, the direct current can be first transformed in an alternative current by collecting the ion current across

a RC circuit with a long time constant. The ionization current is also measured very often by integration method: a capacitance is charged by the ionization current and the voltage change is measured. When the voltage variation reaches a given value, the integrating system is reinitialized. This method allows to follow variations in time of the ionization current.

IV. PROPORTIONAL COUNTERS

A. Principles of operation

1. Gas multiplication

In a proportional counter gas multiplication appears when a high electric field is applied. The principle of operation of these detectors is based on the secondary ionizations created in collisions between accelerated electrons and neutral gas molecules. Further ionizations will then induce new collisions, generating the avalanche. The process terminates when all free electrons have been collected on the anode. The multiplication factor M is usually of many thousands and is kept proportional to the energy deposited by the incident particle. A complete description of the principles of operation is given in reference.[8]

Gas multiplication requires large values of the electric field, of the order of 10^5 V $/cm$ at normal pressure. For this reason the anode is usually a fine wire placed at the center of a cylindrical counter. In such a geometry, the electric field $E(r)$, at distance r from the center of the wire, is given by the equation (15)

$$E(r) = \frac{V}{r\ ln(b/a)} \tag{15}$$

where V is the voltage applied between electrodes, a is the anode radius and b is the inner radius of the cathode. The required large values of E are reached for very low r values, that is in the immediate vicinity of the wire.

Various authors have given analytic formulae to relate the multiplication factor M to the parameters of the detector.[39] Diethorn gives the following expression (16) which assumes a linear relation between the electric field and the first Townsend coefficient (mean number of secondary electrons produced per length unit by a free electron).[40]

$$ln\ M = \frac{V}{ln(b/a)} \frac{ln2}{\Delta V} \left[ln \frac{V}{pa\ ln(b/a)} - lnK \right] \tag{16}$$

where p is the gas pressure, K and ΔV, the potential variation between two successive ionizations, are constants for a given gas. At first approximation the gas multiplication varies exponentially with voltage V. Consequently, the applied voltage must be extremely stable to insure a good energy resolution. For the same reason, the gas pressure must also be very stable. Table 3, a compilation due to Knoll, gives Diethorn parameters for a number of gases.[41]

TABLE 3

Diethorn parameters for different gas mixtures.

Gas mixture	$K \times 10^{-4}$ $(V/cm-atm)$	ΔV (eV)	Reference
$90\%Ar, 10\%CH_4$	4.8	23.6	42
$95\%Ar, 5\%CH_4$	4.5	21.8	42
CH_4 (methane)	6.9	36.5	42
C_3H_8 (propane)	10.0	29.5	42
$96\%He, 4\%C_4H_{10}$ (isobutane)	1.48	27.6	42
$75\%Ar, 15.\%Xe, 10.\%CO_2$	5.45	20.3	42
$69.5\%Ar, 19.9\%Xe, 10.7\%CH_4$	5.45	20.3	42
$64.5\%Ar, 24.7\%Xe, 10.7\%CO_2$	6.0	18.3	42
$90\%Xe, 10\%CH_4$	3.62	33.9	43
$95\%Xe, 5\%CO_2$	3.66	31.4	43

Amplitude of the output pulse is proportional to the collected charge. The expected distribution in the number of electrons produced in an avalanche from a single electron is exponential in shape as given in equation (9). In strong electric fields the electron ionization probability cannot be completely independent of its past history. Finally the overall pulse amplitude distribution approaches a Gaussian shape peak.[44] This amplitude is subject to fluctuations due, like in an ionization chamber, to the number of primary electrons collected, but also to inherent fluctuations of the multiplication factor.[24]

2. Detected signal

The type of analysis developed in section III.A. for ionization chambers can also be applied to proportional counters with several major differences. The whole process develops within a few micrometers from the anode wire. As a result multiplication will take place in a few nanoseconds. Output pulses essentially due to signals induced on the anode by the ions during their fast movement in the region of high electric field, are thus obtained in a very short time, very much shorter than the total drift time. By terminating the counter with a

resistor, one can get a differentiated signal allowing high counting rate capabilities.

B. Gas operation

1. Choice of gas filling

As ionization and avalanche multiplication occur in all gases, the choice of gas filling could be of little importance. For ionization chambers it is somewhat true and the stopping power of the gas determines the choice. In proportional counters appear conflicting experimental requirements: high gain operation, low voltage, high counting rate, good proportionality. The choice will then be between different families of gases, each of them fulfill some of the requirements but not all. The family of noble gases gives avalanche multiplication at lower electric fields. Complex molecules, on the contrary, need much higher values of electric fields since there are many non-ionizing multiplication modes in polyatomic gases. Among these, most used gases are compounds like ammonia, methane, isobutane, carbon dioxide and tetrafluoride. The two families are characterized by a very low electron attachment probability. On the contrary, there exist gas molecules which present a tendency to attach themselves to free electrons, creating negative ions. Halogen gases as well as freons, oxygen and water vapor which have large electron affinities belong to this category.

One will then think to use noble gases for gas filling. However these gases do not allow large gains without entering into a permanent discharge regime. Indeed the excited atoms of these will return to their ground state only by emitting energetic photons which will interact with the cathode, initiating a post avalanche due to extracted photo-electrons. Complex molecules need much higher fields but absorb the photons emitted by the excited atoms, making secondary emission very unlikely. The molecules dissipate the energy either by elastic collisions, either by molecule dissociation or polymerization. The solution which is chosen most of the time is to use a gas mixture, taking

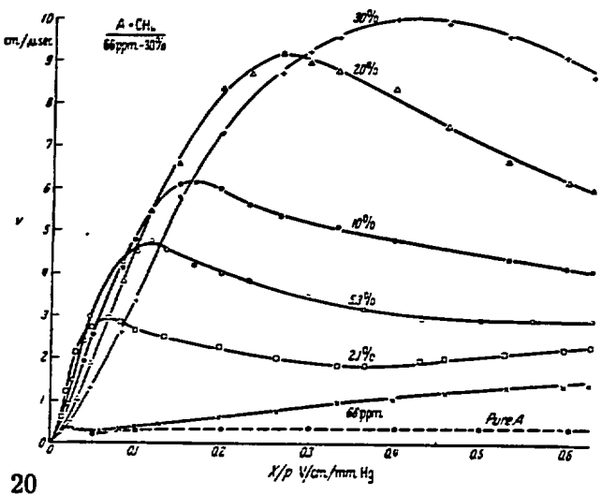

Figure 11. *Drift velocity of electrons in argon-methane mixtures as a function of the reduced pressure expressed in V/cm-torr. From English and Hanna.*[46]

advantage of the low fields needed by noble gases, and of the quenching effect of complex molecules: as metastable level excitations of noble gases lie above the ionization potential of complex molecules, collisions between the two kinds of atoms produce delayed ionization. The charge is then transferred from noble gas to complex molecules. For example, the addition of methane to argon allows to suppress photo-induced effects by absorbing photons, with the other advantage that the electron drift velocity can be drastically increased,[45] as seen in figure 11.[46]

Difficulties can appear after some operation time when products of recombination of complex molecules are polymers. These products will deposit on cathodes and anodes creating a thin isolator layer modifying substantially the way of operation. High densities of charges develop and a permanent discharge is induced. This problem can be solved by adding molecules creating negative ions. It seems obvious to avoid gas molecules which present a tendency to attach free electrons, creating negative ions, (oxygen, water vapor, halogen gases). It means in particular that it is important to prevent the gas filling from being contaminated by air leaks with the outside. However it has been recognized for a long time that the addition of a small quantity of such molecules like ethylic, methylic or isopropylic alcohol has a benefic effect on the ageing of proportional and Geiger-Müller counters.[47] The reason is that alcohol molecules have a low ionization potential and all charges will be finally transferred to these molecules which dissociate when neutralized, avoiding the formation of polymers. Analog qualities are found in a mixture known as the "magic gas" which gives to proportional counters exceptional ageing capabilities. More details on this mixture are given in section IV.C.2.

2. Gas purification

High degree of purity is required in all types of gas counters, since the drift time and signal heights are very sensitive on pollutions, due to effects like scattering, electron attachment and different ionization potentials of the impurities. The most important pollution comes from oxygen, nitrogen or water. On request, quality of commercial gases is usually sufficient but in detectors, impurities come from degassing of molecules adsorbed in chamber materials. Softeners included in many components like plastics, cables and glue are also pollutants.[48] One must also take into account the degradation of organic filling gases under heavy irradiation. For all these reasons it is necessary either to insure a continuous gas renewal, either to recycle the filling gas after purification. Hofmann et al.[48] suggest the use of a combination of Active Carbon, Hydrosorb and Oxisorb cartridges for purification. The sequence of cartridges is important.

3. Gas pressure regulation

Gas renewal implies to keep gas pressure constant with enough precision to maintain

steady multiplication factor in proportional counters and keep energy loss constant enough for Z and energy determination in ionization chambers. There exists a mechanical device in which a volume is enclosed at the given reference pressure. A limber wall of the volume is in contact with the detector volume. A variation in the detector pressure induces deformation of this wall on which a needle is fixed. The needle opens or closes a hole through which gas can enter in the detector to reduce the pressure difference.

A more flexible system consists to compare the detector pressure to a reference pressure (or vacuum) with a sensor. An electronic design allows to open progressive valves either to introduce more gas or to pump the filling gas as shown in figure 12.

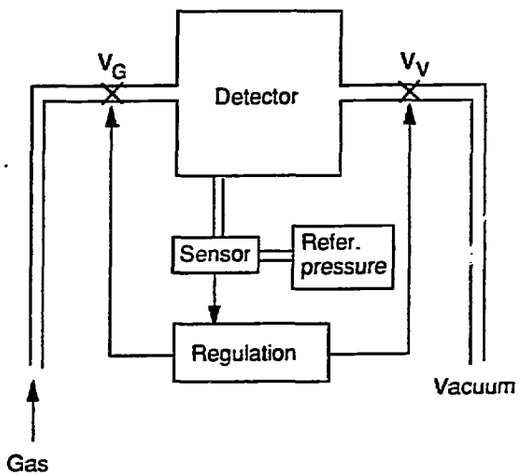

Figure 12. *Principle of operation of an electronic gas pressure regulation.*

A detector can then be maintained at the chosen pressure with a precision of 10^{-3}.

C. Various types of proportional counters

Proportional detectors give high amplitude signals due to the multiplication factor. For this reason they have been used first for energy loss measurements. But because of variations in the gas amplification, the energy resolution is seldom better than a few per cent (20% for protons), and proportional detectors are not competitive with more recent types of detectors. They are much more effective for timing and position determination.[49]

1. Position sensitive proportional counters.

Proportional counters have been widely used to replace nuclear emulsions as active focal plane detectors of magnetic spectrographs. The position resolution is then the most important characteristic. When an incident particle hits a common cylindrical proportional counter, the electrons drift from the place of formation to the anode wire following radial field lines. As the avalanche develops in a very small zone of the wire, the position of the cascade indicates the longitudinal position of the passage of the particle through the detector. A position sensitive

proportional detector can be considered a distributed RC line. A method to get the position on the wire is to observe the relative rise time from signals out of preamplifiers placed at the extremity of the anode wire. Excellent spatial resolutions have been obtained with voltage sensitive preamplifiers by this method introduced by Borkovski and Kopp.[50] However, with this technique, end effects restrict the useful length of the counter.

The most common method of position sensing is the charge division method. The anode is made from high resistive wire so that the collected charge is split between the preamplifiers placed at either end, with an amplitude proportional to the relative position of the avalanche. Different species of resistive wires typically of 20 μm in diameter and of a few hundred Ωcm^{-1} resistivity are used: stainless steel, quartz fiber coated with carbon, or nichrome. The differential linearity will rely on the homogeneity of the wire. The position x, from one edge of the detector, is then calculated by the relation

$$x = L\frac{Q_1}{Q_1 + Q_2} \tag{17}$$

where Q_1, Q_2 are the collected charges on each side of the wire and L its total length. Proper adjustment of gains are needed for optimum resolution.

Various effects contribute to the finite position resolution: electronic noise, thermic noise of the wire, multiple scattering, energy loss fluctuations. Charge preamplifiers used to collect charges do not need to have a good resolution since the electronic noise is negligible as compared to the thermic noise of the resistive wire.

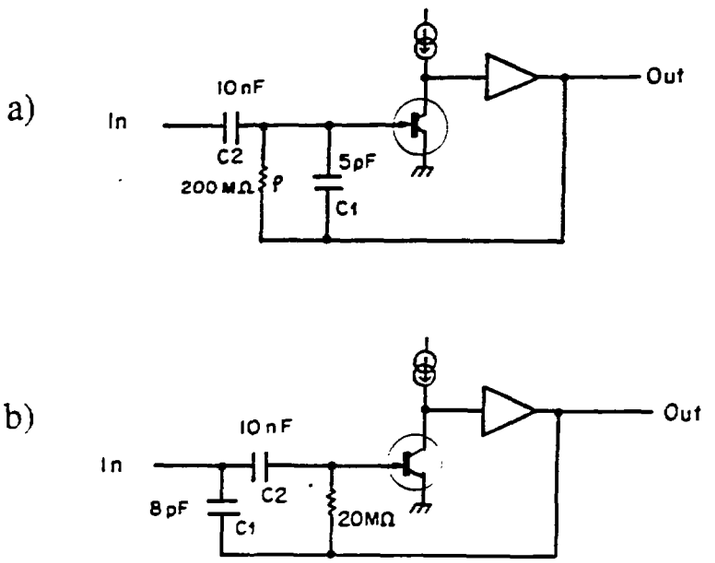

Figure 13. *(a) standard functional diagram of the first stage of a charge preamplifier. (b) actual functional diagram for the particular use of charge division.*

The feed-back resistor ρ of figure 13a can then been reduced by a factor 10 to 20 MΩ in order to eliminate low frequency noises at the entrance of the preamplifier. Nevertheless they must have a good linearity, better than 0.1%. In these working conditions, the voltage variation depends not only on the current collected on the wire but also on the equilibration of capacitive charges through the wire. If for example the wire resistor is $R = 4K\Omega$, the time constant of this contribution is $RC_2/2 = 20\mu s$, low enough to draw a variation of the position determination with the rise time of the pulse. Consequently it is more convenient to work with the design of figure 13b. In this configuration the voltage variation at the exit of the preamplifiers is the product of a function of exponent $2\rho C_1 = 320\mu s$ by a sinusoidal function of period

$$T = \frac{2\pi}{\sqrt{\frac{1}{\rho C_1 R C_2} - \frac{1}{4(\rho C_1)^2}}} = 580\mu s \tag{18}$$

The entrance window gives the main multiple scattering contribution. The effect is emphasized for particles incident upon the counter at a large angle, as usually the case in magnetic spectrometers. As the position is determined by the centroid of the charge distribution deposited by the particle along its trajectory, energy loss fluctuations can also degrade the resolution for large angles.

The FWHM contribution to the limitation in position resolution due to thermic noise is,[51]

$$\frac{\Delta L}{L} \simeq 2.34 \frac{C_S}{Q} \left(\frac{kT}{C}\right)^{\frac{1}{2}} \tag{19}$$

where C is the capacitance of the detector, C_L is the load capacitance, Q is the total charge generated in the detector, k is Boltzmann's constant, T is the absolute temperature and $C_S = C + 2C_L$. Equation (19) shows that the thermic noise contribution decreases for larger collected charges. The combination of all contributions allows to expect resolutions of proportional counters of a few tenths of millimeters.[52] A number of magnetic spectrometers have been equipped with such devices.[23-24,52-55]

2. Multiwire proportional counters.

A proportional counter is useful to detect with a fast response a particle in a limited region of space. The idea to stack together a number of such detectors is not mechanically very attractive so the possibility to put multiwire structures in the same volume of gas was examined. It was thought that such a design could not properly work since the signal obtained on the wire where the avalanche has happened would spread, by capacitive coupling, into all wires. It was the merit of Charpak et al.[56] to demonstrate that the positive induced signals in all neighbouring wires largely compensate the negative signals due to capacitive coupling. A multiwire proportional counter (MWPC) consists of equally distant thin wires sandwiched

between two cathode planes. Each wire can have its own electronic channel. A schematic design is sketched in figure 14.

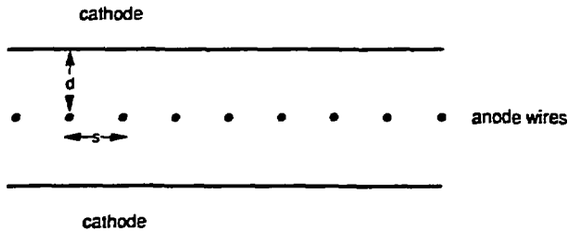

Figure 14. *Schematic diagram of a multiwire proportional counter. A set of parallel wires is mounted symmetrically between two cathode planes. Geometrical parameters s, d are shown.*

Immediately after their discovery, the remarkable properties of these detectors have stimulated systematic studies. Their properties have been extensively investigated, that is efficiency, time resolution, position resolution, as a function of a number of parameters, mechanical dimensions, wire diameter, high voltage, gas mixture.[57]

The properties of such chambers depend strongly on the choice of geometrical parameters. The electrical characteristics, that is electric field variations, capacitance, are determined by the spacing s between anode wires, their radius a and the distance d from the wires to the cathodes. The equation (20) after Erskine gives the capacitance per unit length[58]

$$C = \frac{2\pi\epsilon_0}{(\pi d/s) - ln(2\pi a/s)} \tag{20}$$

This equation (20) shows that the collected charge CV_0 decreases when the wire spacing s decreases. The voltage applied V_0 must be increased to obtain the same gain. For example if s is changed from 2mm to 1mm, V_0 must be multiplied by 1.5 at least, which means more difficulties of operation of the detector. The solution can consist to reduce the wire diameter, but there are obviously mechanical and electrostatic limitations. Practically, good operating conditions are obtained in a 8mm gap, with wires between 10 and $20\mu m$ in diameter and a 2mm spacing.

MWPC have been used from the beginning as position sensitive detectors. The precision was given by the distance between wires. The position in the y direction was obtained with another chamber which anode wires were perpendicular to those of the first chamber. A better two-dimensional position precision can be achieved by measuring the charge distribution induced by the anode avalanche on the cathode plane. Indeed, a large part of the negative signal collected on the anode is not due to electrons but to the drift of positive ions towards the cathode. This movement induces positive signals on all adjacent electrodes. Thus gravity center method gives extremely good localization resolutions. A spatial resolution of 60 μm has been achieved with 400 μm spaced wires.[59] By making cathodes with metallic strips or two perpendicular wire planes, it is possible to obtain the two coordinates of the avalanche in

one MWPC. The resolution in both directions is not equivalent, however much better than the wire spacing because, under moderate gain conditions, the avalanche remains localized at the point where primary electrons reach the wire,[60] and does not surround the anode symmetrically. Therefore, the center of gravity of the induced charge distribution contains information about the position of the original ionization. Further, the ions due to multiplication follow the same electric field lines which terminate where the ionization started.[61]

Multiplication factor and consequently efficiency depend on high voltage and on the filling gas. Systematic studies of operating parameters for different mixtures at various gas concentrations have been accomplished. Position and length of the plateau of $\geq$99% efficiency up to the end of the proportional region, break down voltage, were determined. Studies by Bouclier et al.[57] are represented in figure 15 for argon-isobutane and argon-CO_2 mixtures. Gains up to 10^6 can be reached with argon-CO_2 mixtures. These authors have found that addition of electronegative gas Freon gives remarkable properties to MWPC chambers. With a special mixture named "magic gas" by the authors: argon, 70%, isobutane, 29.54%, 0.46% freon-13B1 (CF_3Br) there are important changes in the behaviour of the detector: gains increase, heavy irradiations induce no change in the characteristics, however no spatial improvements are observed, but time resolution is somewhat degraded.

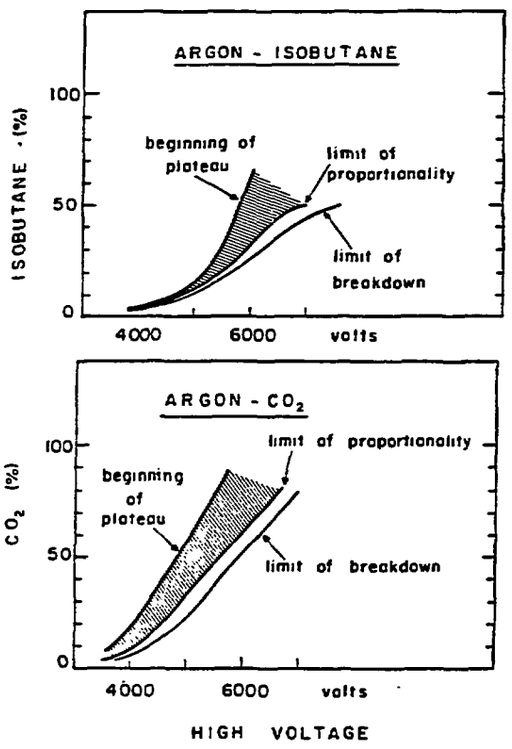

Figure 15. *High voltage plateau and breakdown voltage as a function of CO_2 and isobutane concentration in argon mixtures. From Bouclier et al.*[57]

These detectors were first developed for particle physics experiments, but they have been widely utilized in nuclear physics as position sensitive detectors,[62] many of them in focal planes of spectrometers.[63–65] A cylindrical MWPC with a large solid angle has been built for fission fragment angular distribution studies.[66]They are also very useful for low energy X-rays detection with position readout, allowing quite high counting rates.[67–68] G. Giorginis et al.[69] have built a pressurized Helium MWPC as a neutron polarimeter, using the scattering reaction $(n,^4He)$, the Helium gas serving as target to the neutrons as well as for detection of the He-recoil tracks. They are also widely in use for beam profile measurements of accelerated beams.

3. Detectors operating in the self quenching streamer mode

Systematic studies of proportional chambers led, in certain conditions, to the observation of abnormally large signals. These pulses could not be attributed to a Geiger-Müller mode because their few tens of nanoseconds duration was too short. They were obtained with the argon-isobutane mixture, but with large anode wires. The signals observed had the same characteristics than those found with the "magic gas" described above. Alekseev et al.[70] have shown that both effects belong to a definite operating mode above the proportional region, different from the Geiger-Müller mode, and called the self-quenching streamer mode (SQS). In this process, due the presence of a high electric field, the primary avalanche around the wire develops in a streamer perpendicular to the anode, directed towards the cathode, following the trajectory of primary electrons. The discharge develops till 1 to 3 mm from the anode. It does not result in a spark breakdown because of the quenching effect of the gas which becomes efficient as soon as the weak electric field region is reached. Dimensions of the streamer imply a large number of charges, which explains the difference with the pulse heights of the proportional mode.

The main features are: a very stable operating mode due to a wide efficiency plateau of more than 1000 V, pulses shorter than 200 ns, with a 20 ns rise time, high pulse amplitudes but with a large dispersion, giving a very good signal to noise ratio. Signals depend very little on the primary ionization. Lower mechanical requirements on the geometry make easier the design of large chambers. These interesting characteristics have been widely exploited in particle physics (streamer tubes), but very little in nuclear physic detectors. However multiwire proportional chambers working in the SQS mode have been built for the focal plane of the spectrometer SPES1 at the SATURNE facility,[71] allowing detection of different ions with the same operating conditions, with a spatial resolution of 0.4 mm over a one meter length.

4. Drift chambers.

Multiwire proportional counters achieve excellent position resolution. However in heavy

ion physics many experimentalists prefer to use drift chambers which show several attractive features: a relatively simple and inexpensive design, a reduced mass density, a better differential linearity, the ability to accept a large variety of ion species, precision of the drift distance measurement, some structures display no wires on the ion trajectory.

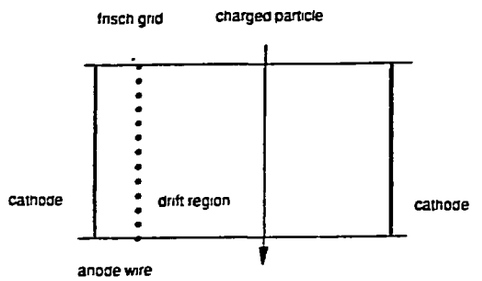

Figure 16. *Schematic drawing of a drift chamber.*

In the simplest design, a drift chamber is constituted of two different parts, as shown in figure 16: a drift region working in the ionization chamber regime and anode wires where avalanche multiplication occurs. A Frisch grid can separate the two regions. Ion-electron pairs created by the particle in the uniform electric field region migrate towards the proportional detection region. The two dimensional localization is given by avalanches on anode wires and by the drift time. This last one is measured between a prompt timing signal derived from an additional timing signal and a pulse collected on one of the electrodes. The avalanche localization is obtained with a proportional resistive wire.[72] In the solution adopted for the spectrometer SPEG at GANIL signals induced by the avalanche on the proportional counter wire are collected on a stripped cathode.[73] Each element of a delay line similar to those described in section V.A. is connected to a strip, and 0.4 mm position has been achieved. However, for large surfaces of detection these designs would lead to uncomfortable working voltages and too long drift times.

Drift chamber structures derived from MWPC consist in a wire plane made of alternating anode and cathode wires corresponding to a number of cells.[74] A delay line connected to the anode wires determines the avalanche anode wire position. This set-up has been adopted for some spectrometer detection systems.[75–77] In the vertical drift chamber of the MIT energy-loss spectrometer, electrons drift from a high voltage cathode plane towards the sense wire. 120 μm position resolution has been obtained, achieving $\Delta p/p \leq 10^{-4}$ requirement.[78] Alternate cathode signals can be bussed out on Odd and Even outputs and coded separately.[77] These arrangements allow to resolve left-right ambiguities, i.e. to distinguish between two tracks located at the same distance from, but on either side of, the anode wire. They allow to reconstruct the incident angle.[79] In another design, in order to get a constant electric field along most of the electron drift trajectory, thus a constant electron velocity, anode wires have

been centered in a symmetric cell limited by cathode wires at a decreasing potential on each side of the anode. [80] All these detectors are of one meter long about.

5. Pictorial drift chambers

In many nuclear physic fields of research, inclusive measurements have proven to be insensitive to underlying reaction mechanism. Exclusive measurements have become a need for a better understanding and have led to the design of 4π detectors, also useful for rare event detection. A solution has consisted to build **streamer chambers** to get high multiplicity reaction details. Within one microsecond after the particle path through the detector, a very high voltage accelerates primary electrons and visible tracks from streamers are obtained. These tracks can be photographed for subsequent analysis. Streamer chambers are limited to a few counts per second. Review papers are given in references.[81–82] Between all 4π detectors designed for high interaction rates, pictorial drift chambers represent probably the most sophisticated gas detectors ever built for nuclear physic experiments.

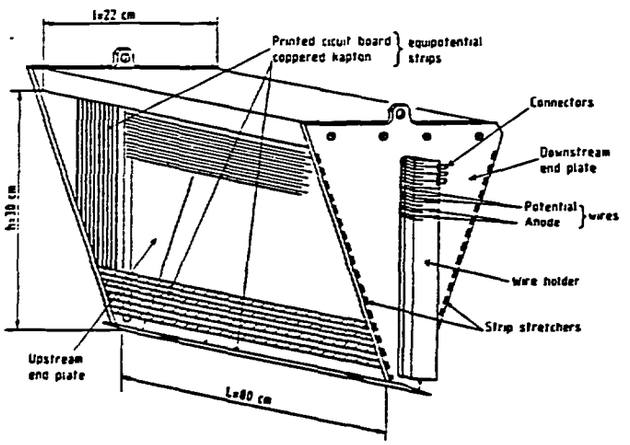

Figure 17. *Drawing of one sector from the PDC DIOGENE in use at SATURNE.*[83]

A pictorial drift chamber consists in a large gas volume of the order of one cubic meter, usually cylindrical in shape, in which ionization electrons drift, under the action of a homogeneous electric field, towards a radial plane of multiplying wires parallel to the beam axis. Like in drift chambers described in section IV.C.3, one gets the position of the particle in one direction by the wire number, and in the other direction, by the drift time. The third coordinate, along the wire, can be given by charge division, as described in section IV.C.1. The energy loss is also determined. Particle identification is obtained by means of energy loss measurement versus momentum analysis from $B\rho$ determination. The large drift time could be inconvenient for high interaction rates, so the detector is divided in several identical sections. Figure 17 shows one of the ten radial sectors from the PDC DIOGENE in use at

SATURNE.[83] Each sector comprises 16 drift cells. A one tesla magnetic field, parallel to the beam axis, allows to determine the magnetic rigidity of the particle. Identification in mass and charge is obtained from the correlation between energy loss and magnetic rigidity.

Some other detectors of this type devoted to nuclear physics have been in operation at TRIUMF,[84] and the BEVALAC.[85] A new 4π detector has been built to be used with the accelerator SIS at GSI: two parts of this detector are pictorial drift chambers. A Central Drift Chamber (CDC) with conical front ends, covering $30^o \leq \theta \leq 160^o$ consists in 16 radial segments;[86] the HELITRON covering $7.5^o \leq \theta \leq 30^o$ consists of 24 radial drift chambers.[87]

V. LOW PRESSURE GAS DETECTORS

A. Parallel plate avalanche chambers.

Parallel plate avalanche counters (PPAC) have been known for many years as a precise timing instrument,[88] but were scarcely used before the considerable development of heavy ion physics, for which gas detectors are better suited. A PPAC consists of two thin parallel stretched foils with a very low gas pressure in between. Particles traverse the detector perpendicular to the planes. The principle of operation is the same as MWPC. The gap between the foils must be small, of a few millimeters, in order to maintain a high electric field, reduce the time spread and get a good time resolution. It has also to be uniform to insure the same operating regime on the whole active surface of the detector. Copper coated epoxy resin for printed circuit board, on which thin metallized (with aluminum or gold) plastic foils are glued, is very well suited for this purpose. The copper layer is used for electric connexions.

These detectors are built to operate with pressures ranging from 1 to 20 millibars. In these low pressure conditions, a voltage of a few hundred volts applied between the plates, typically 300 V/cm-mbar, is sufficient to insure the proportional regime. Released electrons gain enough energy to induce immediate secondary ionization in the homogeneous electric field, and a Townsend avalanche is formed.[14] It seems that pure hydrocarbons are best suited for these detectors and higher gains been reached with isobutane.[89] Multiplication factors of thousands are obtained. 100% detection efficiency can be insured in a wide domain of energy losses. The ΔE energy resolution is limited to about 20% due to straggling in the gas. For large energy losses a pulse height saturation can occur. A 2 to 3 ns rise time pulse is collected due to the high velocity of electrons and the good homogeneity of the electric. Positive ions contribute very little because they are not very close to the anode, in comparison with what

happens in a wire counter. Only the fast component of the signal due to the motion of electrons is used. The slow part from the positive ions is eliminated by differentiation of the signal. Best timing performance may not necessarily correspond to the fastest output rise time, since at very low gas pressure, pulse fluctuations can become important.[90] Time resolutions better than 200 ps (fwhm) have been obtained with such detectors even in large dimensions.[91] Of course a delay of 40 to 50 ps/ cm from the propagation time of signals along the electrodes has to be taken into account.[90]

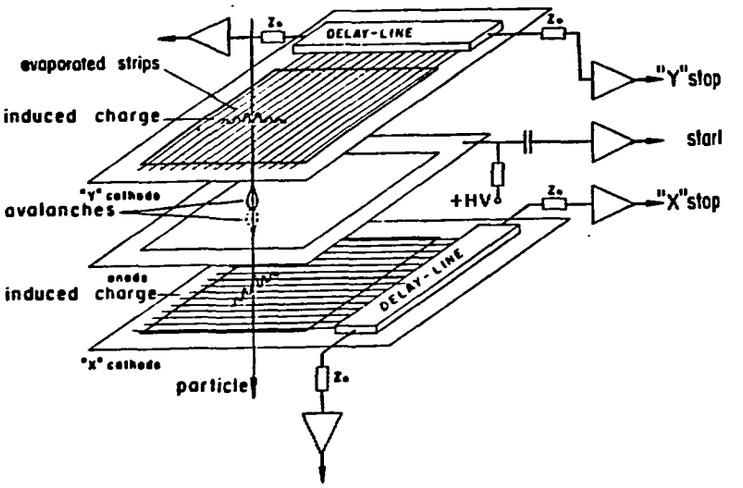

Figure 18. *Schematic diagram by Breskin and Zwang of localization by strips on cathodes in a PPAC. Fast delay lines allow to reconstruct the center of gravity of induced charges.*[92]

It is possible to achieve a very good spatial resolution with avalanche parallel plate detectors. The localization is realized by strips on cathodes and by using fast delay lines to reconstruct the center of gravity of induced charges, as illustrated by figure 18.[92] For example, figure 19 shows a graph where a resolution better than 300 μm has been obtained with a 2 mm wide strip detector operating at 10 mbar isobutane pressure irradiated by 84 Mev oxygen ions.[93]

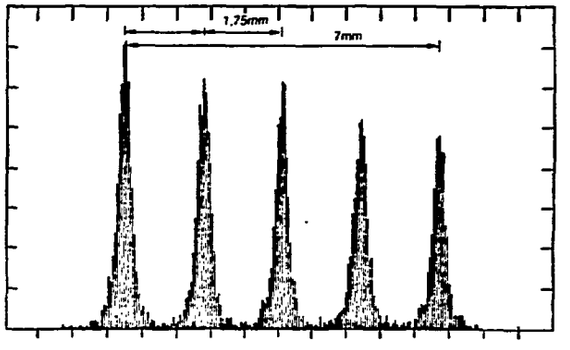

Figure 19. *Pulse height distribution of 84 MeV oxygen ions through 200 μm slits in a PPAC equipped with 2mm wide strips. With courtesy of Gaiardo et al.*[93]

Position resolution depends on electronics of course, but also on the quality of the delay line. This is true not only for PPAC but also for drift chambers already described. Most authors use manufactured delay lines. Some authors have obtained better results with electromagnetic delay lines they have built.[93] The delay line made by the authors from figure 19 is composed of simple $LC_p - C_s$ circuits as shown in figure 20. The conception of inductive elements L is important to get a low dispersion delay line.[94] They are made of a continuous winding on a threaded plastic rod having taps every 3 to 5 windings to constitute individual cells. Impedances of the order of 100Ω are obtained with a few nanosecond delay per element. The capacitor C_s eliminates the overshoot of the pulse collected at the end of the line, due to mutual inductance between cells. This capacitor C_s is detector dependent because the total capacitance takes into account the capacitance of the detector. These delay lines have a better rise time, a higher impedance and less amplitude attenuation than commercial ones. For example an attenuation factor less than 2 is obtained in a detector equipped with a 75 cm line of 400 ns total delay and 15 ns rise time.[55] A careful construction of the induction elements and a selection of capacitors give a good differential linearity. Nonlinearities smaller than 1% have been reached for a drift chamber in the focal plane of the spectrometer SPEG at GANIL.[73]

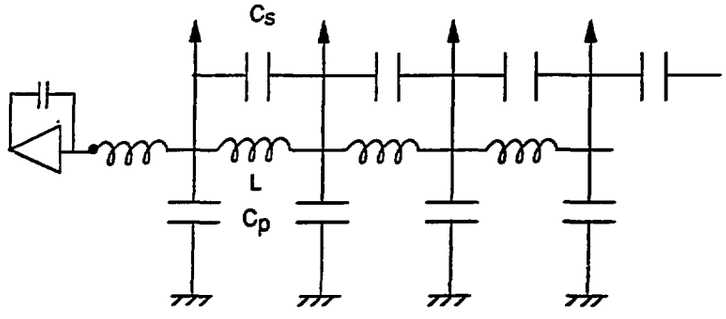

Figure 20. *Drawing of a delay line. Capacitors C_S take into account the detector capacitance.*

PPAC are extensively used as first detectors in many experimental equipments to get a timing signal. They possess a number of attractive features: these detectors are not sensitive to radiation damage, no sparks coming from wires, the fast removal of positive ions gives them a high rate capability, as position detectors they have the advantage on MWPC the absence of wires on the ion trajectories. Their low operation gas pressure allows the use of very thin windows, which renders PPAC the thinnest available timing and position sensitive detectors. These properties have found specific applications in heavy ion experiments, essentially for ray tracing.[95-99] As they can be built in large dimensions, not influenced by strong magnetic fields, they are used very often in focal plane of spectrometers.[23,31,55]

B. low pressure multiwire proportional counters

It has been shown that a very good time resolution is achieved in very low pressure proportional counters, due to the fast drift velocity of electrons. Breskin has demonstrated that at pressures of the order of 1 mbar or less, multiplication happens in two steps.[100] A first amplification takes place in the almost constant field region, like in parallel plate avalanche counters described in the preceding section. A second amplification happens, like in a high pressure MWPC, around the wire where values of 10^5 Volts/cm.torr are reached. In this large electric field ions recoil with velocities larger than 10^6 cm/s. As a result, the time distribution of the ion induced signal is divided in two parts: a very fast one mixed with the electronic signal and a slower one due to the ion drift in the constant electric field region.[101] The variation of the time distribution signal with gas pressure is illustrated in figure 21.

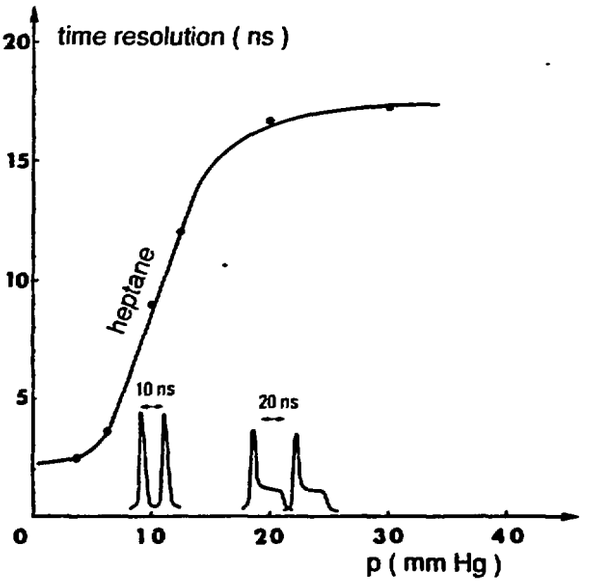

Figure 21. *Variation with heptane gas pressure of the time distribution signals in a low pressure MWPC.*[101] *Represented signal shapes correspond to 3 torr and 25 torr respectively. From Binon et al.*

At 3 torr, the pulse time distribution is symmetrical in shape due to the very fast collection of ions on the cathode. At 25 torr the tail of the pulse is due to the ion drift induced signal. Consequently, the best time resolution is obtained at low gas pressure, where the rise time is shorter. At a 2 torr gas pressure, a very good time resolution of 100 ps has been achieved by Breskin et al.[102] Excellent spatial resolutions can be found; a $80\mu m$ FWHM resolution has been reached with a counter in which electrodes were wound with a space of 2 mm.[103]

C. Low pressure multi-step detectors

Multi-step detectors are used for imaging in many fields of research or in applied physics.[104–106] The mechanism of these detectors is based on a preamplification of the initial charge and the transfer of the primary avalanche to a secondary amplification step. They are used in nuclear physics for the detection of low energy heavy ions. Nuclei of A $\geq$ 100 and 10 MeV total kinetic energy are produced in fusion reactions, studied at energies close to the coulomb barrier. Indeed window thickness of 1 μm is required, which limits the gas pressure of gaseous counters to 1 or 2 mbar. At these considered energies, electronic energy loss is low and only a few tens of electrons will be created in the low pressure detector. Even PPAC or MWPC are excluded because of insufficient amplification gain. Breskin et al.[107] have studied a multi-step detector able to satisfy this particular need. The preamplification step operates in the PPAC mode. When used at normal pressure, a transfer region to the second amplification zone is essential for the absorption of the photons produced in the gas mixture. At low gas pressure, electron diffusion leads to wide avalanches, giving efficient transfer process. Further the quenching efficiency of isobutane renders optional the transfer region which may degrade the good timing properties of the detector. In the Breskin device the second amplification stage is a MWPC. This detector gives good timing resolution (150 ps at FWHM), 200 μm position resolution, and was fully efficient for the detection of ^{160}Gd nuclei with kinetic energy down to 1.3 MeV.

VI. GAS MICROSTRIP DETECTORS

A. Description

A microstrip gas chamber (MSGC) is a proportional counter in principle. This device could appear thanks to the development of microelectronic technology. In some way it reproduces the field structure of multiwire chambers, but at a much smaller scale and interesting specific designs. It consists in a sequence of alternating very thin metal anodes of a few μm width and cathode strips, etched with high accuracy on an isolating substrate, as represented in figure 22.[108] With this technology, each cell can be 200 μm wide and less. These detectors are made using electron beam lithography for the mask scribing and photolithography and thin film deposition to engrave the electrodes. A deposit of metal on the backplane defines a back cathode. The entrance window in front can also serve as cathode, to transport primary electrons generated by ionization towards the thin anode where multiplication occurs.

The first detector of this type was built by Oed who introduced the idea and demonstrated its qualities as low energy alpha and proton detector.[109] The mode of operation of this device is the following: a drift electrode defines a zone of charge collection of a few millimeter thickness, then field lines connecting the drift and back cathode to the anode, concentrate

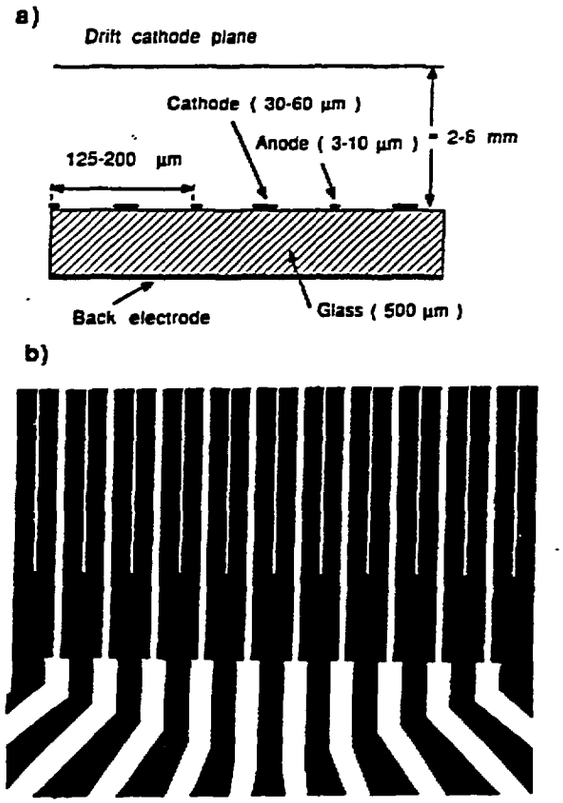

Figure 22. *a) schematic cross section of a microstrip gas detector designed by Angelini et al.*[108] *b) Anode-cathode structure of the detector. The substrate is represented in black.*

on the thin anode strips at a positive potential with respect to the broader cathode strips, resulting in a high electric field of 50 kV/cm or more in their neighbourhood. Due to the low width of the anode and the small anode-cathode separation, few hundred volt operation only insure the proportional regime mode with gains of thousands. The ions produced around the anode are captured rapidly by the cathode strip at a distance of 50μm only. Many laboratories have started to study in detail properties of these detectors as a function of the gas filling, the nature of substrate and of electrodes.

Gas mixtures for MWPC can also be used for these detectors operating at a normal pressure. For a better efficiency it is suitable to fill the device with dense gases in which the energy loss is increased, to compensate small drift gaps necessary to get fast drift and minimize parallax error for localization accuracy. Especially, pure isobutane, argon and xenon mixed with quenching gases are most suitable. After irradiation, a gain modification very localized to the region of irradiation has been attributed to the well known ageing of gaseous counters, that is deposits on anode strips. This phenomenon has been observed in all mixtures

by Bouclier et al.[110] except for the mixture 93% argon, 7% DME (dimethyl ether) for which no visible deposit could be found.

B. Influence of the substrate and nature of electrodes

The substrate should be good enough isolator to insure a correct potential distribution. At the same time, it has to be conducting enough to evacuate charges arising from ions formed in avalanche near anodes. Barasch et al.[111] estimate $10^{13}\Omega/cm^2$ as an optimal value for particle fluxes of $10^5 cm^{-2}s^{-1}$ and a gas gain of about 10^4. It is not obvious to find a material which corresponds to this requirement. Glasses or plastics exhibit much higher resistivities, and when they are loaded with conductive materials, it is difficult to obtain the required resistivity. In place one finds an inhomogeneous mixture of microscopic conducting and dielectric phases.

Glass supports have been used at first. But, after a few hours of operation, a drop of gain is observed, independent of the irradiation rate, accompanied with an energy resolution degradation.[110] When switching off the high voltage the gain restores its initial value after a few hours. This effect may be interpreted by a variation of ionic conductivity in glass due to the motion of alkali ions. With potential, as ions migrate in the bulk material, the number of current carriers decreases with time, resulting in an increase of resistivity. This effect can be reduced by a repulsion of ions with the rear potential. In fact this method is effective only for thin substrates. A solution has consisted in using electronic conductivity glasses with a low proportion of alkali like Murano glass or various Corning glass samples selected by some authors. On the other hand plastics like Kapton, Kevlar,[110] and polyurethane copolymer,[111] seem to be suitable supports for MSGC, being mechanically stable, with good surface quality and required bulk resistivity.

A way to solve surface charging up effects is to make the surface become somewhat conductive by ion implantation or by thin film deposit. For example, adequate stability has been obtained on highly isolating quartz by implantation of 5.10^{16} Boron ions/cm^2.[112] A quite different method employed by Angelini et al.[113] consisted in using amorphous low resistivity silicon wafer as substrate. The isolation between anode and cathode is provided by a $2\mu m$ thick thermal oxide layer. This technique seems very promising,[114] and multi-chip technology may well be the next step of development.[115] Devices with such thin dielectric substrates allow interesting features as described in section VI.C.

With such thin anodes, the potential difference is somewhat limited because of sparks at the edges provoked by the high field strength. As the heat capacity of a few μm wide strip is limited, the spark can melt or even evaporate the anode. For this reason the layer thickness should be of 1 μm thick at least, with the other advantage to provide a low strip resistance, essential for a short rise time of the signal. Skillfully chosen structure shapes like those

represented in figure 23 make possible to keep the field strength in the parallel sections higher than in any other part of the strips.[116]

To avoid uncontrollably charges on the isolating part, at least 50% of the substrate surface should be covered with metal. Deposits of aluminum, chromium, and gold are used. The two first ones form protective oxide layer which can eventually lead to breakdown effects.

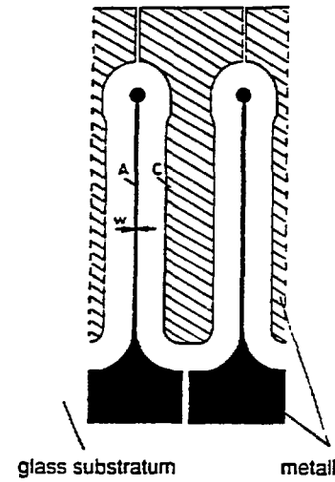

Figure 23. *Structure shape of electrodes designed by Oed et al.*[116] *allowing a 10^5 gas amplification.*

C. Performances

These detectors are very promising and should allow the development of new types of experiments in nuclear physics.

The high precision geometry of anodes made with 0.1 μm definition by microelectronic techniques, results in uniform gas amplification on the entire surface. Therefore one can expect a much better energy resolution than obtained with wire proportional counters. However, amplitude of signal is limited by avalanche amplification gain not likely to exceed 10^4, because of spark breakdown. The compact configuration of the device and eventually the

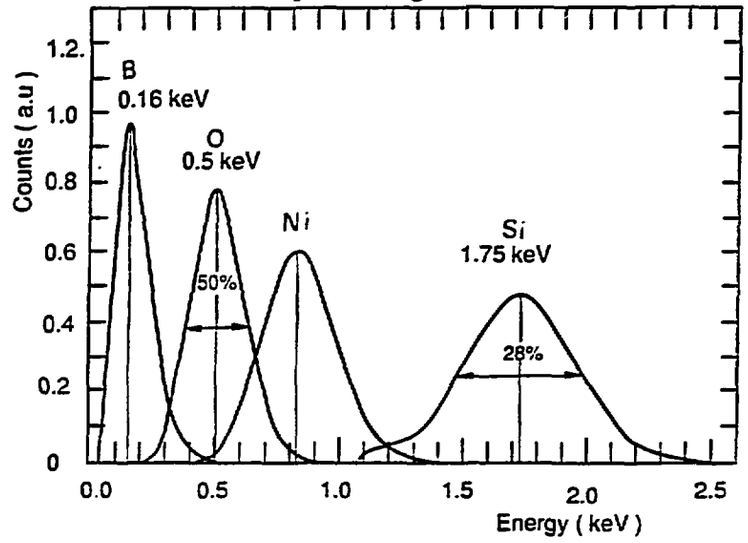

Figure 24. *Pulse height distribution of very low energy X-rays obtained with a microstrip gas detector.*[117]

high dielectric constant of substrate result in a high capacitive load, that is a high noise level in the charge sensitive preamplifiers. Thus, energy resolution can be limited by the signal-to-noise ratio. This resolution is about 12% at 5.9 KeV.[108] Figure 24 shows low energy X-ray spectrum from a detector for the SODART telescope.[117]

The main interesting property of these detectors is their good granularity due to very small spacing, ensuring a high localization accuracy. Systematic errors originating from the position of strips can be neglected. Various authors have found excellent resolutions $\sigma = 30\mu$m for tracks perpendicular to the surface.[118] This result is obtained by calculating the center of gravity of signals given by primary electrons spreading by diffusion over two or three strips. Induced signal due to collection of positive ions on the back electrode can be exploited for two-dimensional read-out.[119] The signal amplitude depends on the thickness of dielectric substrate. It is then advantageous to use a design like the one used by Angelini et al.[113] in which the isolation is provided by a 2 μm thick thermal oxide layer only. However, the large distance between anode and backplane give a very small signal on the back electrode, electrically shielded by the much closer cathodes. In new devices this distance has been reduced to the thin silicon oxide layer of 2 μm ,[120] so a large fraction of the charge delivered in the avalanche is induced on the back electrode almost free of shape. Figure 25 represents

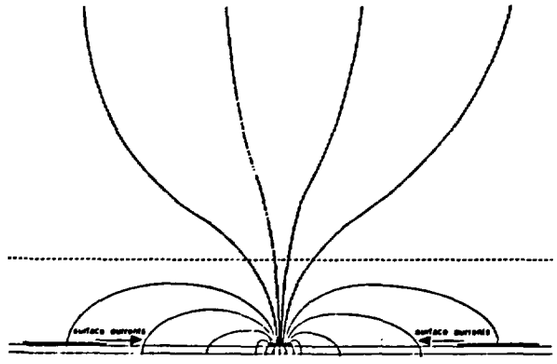

Figure 25. *Representation of electric field lines in a MSGC with a thin substrate inducing signals on the back cathode.*[114]

the electric field lines with a thin substrate. The back electrode can then be split in as many strips as wanted to make a true high resolution two-dimensional device, or even divided in square pads separated by a few μm making a pixel structure.[121] Spatial resolutions of 30μm for both coordinates is expected in the future.

The fast ion collection allows high flux irradiation. Rate capabilities of the order of 10^5 particles/mm^{2}s have been achieved,[110,112–113,121] with a small decrease of the amplification gain for some devices. As we have seen, these counters present many advantages as compared to the existing detectors and if they can be built in large dimensions,[122] they will find many applications in the future: spatial geometry ten times smaller than MWPC, which means

a position resolution improved by an order of magnitude, low voltage of operation, fast collection, high counting rate, high radiation resistance, low cost, mechanical stability.

VII. CONCLUSION.

In the 1970's the combination of electronic improvements, discovery of multiwire proportional detectors, and the huge development of heavy ion physics have made gas detectors between the most suited types of detectors in nuclear physic experiments. Developments of various kinds of very competitive detectors have appeared during the next ten years: energy, position and timing detectors, sectorized ionization chambers... At the same time, processes involved in gas detectors have been extensively studied and are now well understood. Studies on gas filling have resulted in the discovery of interesting mixtures increasing the capabilities. Nowadays, gas detectors are used most often in combination with solid type detectors in complex designs allowing complete identification of reaction products, sometimes in 4π equipments. New devices are continuously appearing in publications. For example, proceedings of the Sixth International Wire Chamber Conference held in Vienna in 1992, contain about one hundred communications.[123] In particular, microstrip gas detectors will certainly know important developments in a near future.

The author wish to thank J. Guillot and L. Tassan-Got for helpful discussions and a careful reading of the manuscript.

1. Fano U., Penetration of protons, alpha particles, and mesons, *Ann. Rev. Nucl. Sci.*, **13**, 1, 1963.

2. Ahlen S. P., Theoretical and experimental aspects of the energy loss of relativistic heavily ionizing particles, *Rev. Mod. Phys.* **52**, 121, 1980, and references therein.

3. Northcliffe L. C. and Schilling R. F., Range and stopping power tables for heavy ions, *Nucl. data tables* **A7**, 233, 1970.

4. Ziegler J. F., *Handbook of stopping cross sections for energetic ions in all elements*, Pergamon, New York, 1980.

5. Hubert F., Bimbot R., and Gauvin H., Range and stopping power tables for 2.5-500 MeV/u heavy ions in solids, *At. Data and Nucl. Data Tables* **4**, 1, 1990.

6. Geissel H., Laichter Y., Schneider W. F. W., and Armbruster P., Energy loss and energy loss straggling of fast heavy ions in matter, *Nucl. Instr. and Meth.* **194**, 21, 1982.

7. Herault J., Bimbot R., Gauvin H., Kubica B., Anne R., Bastin G., and Hubert F., Stopping powers of gases for heavy ions (O, Ar, Kr, Xe) at intermediate energy. Vanishing of the gas solid effect, *Nucl. Instr. and Meth.* **B61**, 156, 1991.

8. Sauli F., Principles of operation of multiwire proportional and drift chambers, CERN/77-09, Geneva, 1977.

9. Ermilova V. C., Kotenko L. P., and Merzon G. I., Fluctuations and the most probable value of relativistic charged particle energy loss in thin gas layers, *Nucl. Instr. and Meth.* **145**, 555, 1977.

10. Landau L. M. and Lifshitz E. M., *Electrodynamics of continuous media*, Addison -Wesley, Reading, Mass. USA, 1960, chap. 12.

11. Vavilov P. V., Ionization losses of high energy heavy particles, *Zh. Eksp. Teor. Fiz.* **32**, 920, 1957, *Sov. Phys. JETP* **5**, 749, 1957.

12. Igo G. J., Clark D. D., and Eisberg R. M., Statistical fluctuations in ionization by 31.5 MeV protons, *Phys. Rev.* **89**, 879, 1953.

13. Schultz G., Charpak G., and Sauli F., Mobilities of positive ions in some gas mixtures used in proportional and drift chambers, *Rev. Phys. appliquée*, **12**, 67, 1977.

14. Townsend J., *Electrons in gases*, Hutchinson, London, 1947.

15. Price W. J., *Nuclear radiation detection* Mc Graw-Hill, New York, 1958.

16. Rossi B. and Staub H., *Ionization chambers and counters*, Mc Graw-Hill, New York, 1949.

17. Wilkinson D. H., *Ionization chambers and counters*, Cambridge University press, Cambridge, 1950.

18. Fulbright W., *Ionization chambers in nuclear physics*, Handbuch der Physik, Springer-Verlag, Berlin, 1958, vol 45.

19. Buneman O., Cranshaw T. E., and Harvey J. A., Design of grid ionization chamber, *Can. J. Res.*, **27A**, 191, 1949.

20. Naulin F., Roy-Stéphan M., and Kashi E., Improved energy resolution in an ionization chamber through suppression of the electrical field distorsions, *Nucl. Instr. and Meth.* **180**, 647, 1980.

21. Simon G., Trochon J., Brisard F., and Signarbieux C., Pulse-height defect in an ionizaton chamber investigated by cold fission measurements, *Nucl. Instr. and Meth.* **A286**, 220, 1990.

22. Erskine J. R., Braid T. H., and Stoltzfus J. C., An ionization chamber type of focal plane detector for heavy ions, *Nucl. Instr. and Meth.* **135**, 67, 1976.

23. Tassan-Got L., Stéphan C., Bizard G., Duchon J., Laville J. L., L'Haridon M., and Louvel M., Heavy ion identification system for a magnetic spectrometer, *Nucl. Instr. and Meth.* **200**, 280, 1982.

24. Saghai B. and Roussel P., Compteur proportionnel à localisation pour la détection des ions lourds, *Nucl. Instr. and Meth.* **141**, 93, 1977.

25. Rozet J. P., Chetioui A., Piquemal P., Vernhet D., Wohrer K., Stéphan C., and Tassan-Got L., Charge-state distributions of few electron ions deduced from atomic cross sections, *J. Phys. B.* **22**, 33, 1989.

26. Pfützner M., Geissel H., Brohm Th., Magel A., Münzenberg G., Nickel F., Scheidenberger C., Schmidt K. H., Sümmerer K., Vieira D., and Voss B., Energy deposition of relativistic heavy ions in an ionization chamber at the FRS, *GSI scientific report 1991*, Darmstadt, 1992.

27. Badhwar G. D., Calculation of the Vavilov distribution allowing for electron escape from the absorber, *Nucl. Instr. and Meth.* **109**, 119, 1973.

28. Schapira D., Teh K., Blankenship J., Burks B., Foutch L., Kim H. J., Korolija M., McConnell J. W., Messick M., Novotny R., Rentsch D., Shea J., and Wieleczko J. P., The HILI a multidetector system for light ions and heavy ions, *Nucl. Instr. and Meth.* **A301**, 76, 1991.

29. Sann H., Damjantschitsch H., Hebbard D., Junge J., Pelte D., Povh B., Schwalm D., and Tran Thoai D. B., A position sensitive ionization chamber, *Nucl. Instr. and Meth.* **124**, 509, 1975.

30. Bocquet J. P., Brissot R., and Faust H. R., A large ionization chamber for fission fragment nuclear charge identification at the Lohengrin spectrometer, *Nucl. Instr. and Meth.* **A267**, 466, 1988.

31. Gardes D., Monnet F., Barbey S., Borderie B., Dumail M., Gobbi A., Rivet M. F., and Volkov P., a sectorized ionization chamber: the MEΩ detection system, *Nucl. Instr. and Meth.* **A247**, 347, 1986.

32. TP-MUSIC III- A new tracking detector for the ALADIN facility, Meijer R. J., Liu Z. A., Lühning J., Lynen U., Sann H., and Quick W., *GSI scientific report 1989*, Darmstadt, 1990.

33. Gruhn G. R., Binimi M., Legrain R., Loveman R., Pang W., Roach M., Scott D. K., Shotter A., Symons J., Wouters J., Zisman M., Devries R., Peng Y. C., and Sonheim W., Bragg curve spectroscopy, *Nucl. Instr. and Meth.* **196**, 33, 1982.

34. Schiessl C., Wagner W., Hartel K., Kienle P., Kvrner H. J., Mayer W., and Rehm K. E., A Bragg-curve spectroscopy detector, *Nucl. Instr. and Meth.* **192**, 291, 1982.

35. Asselineau J. M., Duchon J., L'Haridon M., Mosrin P., Regimbart R., and Tamain B., Performance of a Bragg curve detector for heavy ion identification, *Nucl. Instr. and Meth.***204**, 109, 1982.

36. Cebra D. A., Howden S., Karn J., Kataria D., Maier M., Nadasen A., Ogilvie C. A., Stone N., Swan D., Vander Molen A., Wilson W. K., Winfield J. S., Yurkon J., and Westfall G. D., Bragg curve spectroscopy in a 4π geometry, *Nucl. Instr. and Meth.* **A300**, 518, 1991.

37. Gramegna F., Prete G., Viesti G., Iori I., Moroni A. and Ghinelli F., Bragg curve spectroscopy at high rates, *Nucl. Instr. and Meth.* **243**, 601, 1986.

38. Mittig W.L., Gillibert A., Juzans P., Schutz Y., Stéphan C., Tassan-Got. L., and Villari A. C. C., unpublished data, 1989.

39. Shalev S. and Hopstone P., Empirical expressions for gas multiplication in ^3He proportional counters, *Nucl. Instr. and Meth.* **155**, 237, 1978.

40. Diethorn W., A methane proportional counter system for natural radiocarbon measurements, USAEC/NYO-6628,1956.

41. Knoll G. F., *Radiation detection and measurement*, Wiley and sons, New York, USA, 1979.

42. Wolff R. S., Gas constants for various gas mixtures, *Nucl. Instr. and Meth.* **115**, 461, 1974.

43. Hendricks R. W., Space charge effects in proportional counters, *Rev. Sci. Instr.* **40**, 1216, 1969.

44. Genz H., Single electron detection in proportional gas counters, *Nucl. Instr. and Meth.* **112**, 83, 1973.

45. Va'vra J., Wire chamber gases, *Nucl. Instr. and Meth.* **A323**, 34, 1992, and references therein.

46 . English W. N. and Hanna G. C., Grid ionization chamber measurement of electron drift velocity in gas mixtures, *Can J. Phys.*, **31**, 768, 1953.

47. Grunberg C., Cohen L., and Mathieu L., Multiwire proportional and semi-proportional counter with a variable sensitive volume, *Nucl. Instr. and Meth.* **78**, 102, 1970.

48. Hofmann Th., Lynen U., and Sann H., Gas purification for the TP-MUSIC detector, *GSI scientific report 1991*, Darmstadt, 1992.

49. Ford Jr J. L. C., Position sensitive counters as focal plane detectors, *Nucl. Instr. and Meth.* **162**, 277, 1979.

50. Borkovski C. J. and Kopp M. K., New type of position sensitive detectors of ionizing radiation using rise time measurement, *Rev. Sci. Instr.* **39**, 1515, 1968.

51. Markham R. G. and Robertson R. G. H., High resolution position sensitive proportional counter, *Nucl. Instr. and Meth.* **129**, 131, 1975.

52. Miller G. L., Williams N., Senator A., Stengaard R., and Fischer J., A position sensitive detector for a magnetic spectrograph, *Nucl. Instr. and Meth.* **91**, 389, 1971.

53. Fulbright H. W., Markham R. G., and Lanford W. A., position sensitive particle detectors used in a magnetic spectrometer, *Nucl. Instr. and Meth.* **108**, 125, 1973.

54. Hafner H., and Duhm H. H., The 1.4 m ΔE-E range position sensitive detector of the Heidelberg Q3D magnetic spectrograph, *Nucl. Instr. and Meth.* **160**, 273, 1979.

55. Bianchi L., Fernandez B., Gastebois J., Gillibert A., Mittig W., and Barrete J., SPEG: An energy loss spectrometer for GANIL, *Nucl. Instr. and Meth.* **A276**, 509, 1989.

56. Charpak G., Bouclier R., Bressani T., Favier J., and Zupancic C., The use of multiwire proportional counters to select and locate charged particles, it Nucl. Instr. and Meth. **62**, 262, 1968.

57. Bouclier R., Charpak G. Dimcovski Z., Fischer G., Sauli F., Coignet G and Flügge G., Investigation of some properties of multiwire proportional counters, *Nucl. Instr. and Meth.* **88**, 149, 1970.

58. Erskine G. A., Electrostatic problems in multiwire proportional chambers, *Nucl. Instr. and Meth.* **105**, 565, 1972.

59. Frieze W., Dhawan S., Disco A. A., Fajardo L., Majka R., Marx J. N., Nemethy P., Sandweiss J., and Slaughter A., A high resolution multiwire proportional chamber system, *Nucl. Instr. and Meth.* **136**, 93, 1976.

60. Sauli F., Limiting accuracies in multiwire proportional and drift chambers, *Nucl. Instr. and Meth.* **156**, 147, 1978.

61. Sanada J., Growth of the avalanche around the anode wire in a gas counter, *Nucl. Instr. and Meth.* **196**, 23, 1982.

62. Ford T. D., Needham G. A., Brady F. P., Romero J. L., and Castadena C. M., A multiwire chamber system for measurements of charged particle spectra, *Nucl. Instr. and Meth.* **228**, 81, 1984.

63. Ball G. C., Multiwire proportional chamber focal plane detector systems with digital readout, *Nucl. Instr. and Meth.* **162**, 263, 1979.

64. Chalupka A., Bartl W., Schönauer l., Bahnsen K. U., Labedzki H. J., Scheerer H. J., Vonach H., and Ziegler G., New MWPCs for the Munich Q3D spectrograph, *Nucl. Instr. and Meth.* **217**,113, 1983.

65. Cunningham R. A., Sanderson N. E., Snodgrass W. N. J., Banes D. W., Hoath S. D., and Mo J. N., Construction and performance of a multiparameter focal plane detector for use on a QMG/2 magnetic spectrometer, *Nucl. Instr. and Meth.* **A234**, 67, 1985.

66. Glässer P., Rösler H., Männer R., and Specht H. J., A position sensitive multiwire proportional chamber for fission fragments with large solid angle, *Nucl. Instr. and Meth.* **141**, 111, 1977.

67. Dangendorf V., Bethge K., Kelbch C., Kelbch S., Ullrich J., and Schmidt-Bvcking H., Position sensitive gas proportional counter with good time resolution for low energy X-ray detection, *Nucl. Instr. and Meth.* **A243**, 465, 1986.

68. Dmitriev G. D. and Frumkin I. B., A study of MWPC accuracy of X-ray coordinate sensing at high counting rate, *Nucl. Instr. and Meth.* **A295**, 384, 1990.

69. Giorginis G., Wochele J., Kiontke S., Maschuw R., and Zeitnitz B., A three dimensional He-recoil MWPC for fast polarized neutrons, *Nucl. Instr. and Meth.* **A251**, 89, 1986.

70. Alekseev G. D., Kalinina N.A., Karpukhin V. V., Khazins D. M., and Kruglov V. V., Investigation of self quenching streamer discharge in a wire chamber, *Nucl. Instr. and Meth.* **177**, 385, 1980.

71. J.Guillot, M.Morlet, A. Willis, M. Denoit, R. Sellem, J.Beaunier, Y. Bisson, G. Chesneau, G.Goby, P.Lelong, R.Margaria, A.Maroni, P.Menny, D.Seguy, P.Volkov, the SPES1 chambers at SATURNE, *private communication*

72. Fuchi Y., Tanaka M. H., Kubono S., Kawashima H., Takaku K., and Ichihara T., Development of detectors for the second focal plane of SMART, RIKEN accel. Prog. rep. **25**, 129, 1991.

73. Villari A. C. C., Mittig W., Blumenfeld Y., Gillibert A., Gangnant P., and Garreau L., A test of new position sensitive detectors for SPEG, *Nucl. Instr. and Meth.* **A281**, 240, 1989.

74. Walenta H. A., Heintze J., and Schürlein B., The multiwire drift chamber, a new type of proportional wire chamber, *Nucl. Instr. and Meth.* **92**, 373, 1971.

75. Atencio L. G., Berg G. P. A., Von Brentano P., Brinkmvller B., Hlawatsch G., Meissburger J., Moore C. F., Morris C. L., Paul D., Rsmer J. G. M., Rogge M., Von Rossen P., Sagefka T., Seestrom-Morris S. J., and Zemlo L., The new focal plane detector for the magnet spectrometer Big Karl, *Nucl. Instr. and Meth.* **A242**, 95, 1985.

76. Engelage J., Baumgartner M. E., Beleal E., Berman B. L., Bieser F., Brady F. P., Bronson M., Carroll J. B., Crawford H. J., Flores I., Greiner D. E., Greiner L., Hashimoto O., Igo G., Kadota S., Kirk P. N., Lindstrom P. J., McParland C., Nagamiya S., Olson D. L., Porter J., Romero J. L., Ruiz C. L., Symons T. J. M., Tanahita I., Wada R., Webb M. L., Yamada J., and Yee H., Design of the BEVALAC heavy ion spectrometer system and its performance in studying ^{12}C fragmentation, *Nucl. Instr. and Meth.* **A277**, 431, 1989.

77. Henderson R. S., Hausser O., Hicks K., Gunther C., Faszer W., Sawafta R., and Poppe N., Large area horizontal drift chambers for a focal plane polarimeter at the TRIUMF medium resolution spectrometer, *Nucl. Instr. and Meth.* **A254**, 61, 1987.

78. Bertozzi W., Hynes M. V., Sargent C. P., Creswell C., Dunn P. C., Hirsch A., Leitch M., Norum B., Rad F. N., and Sasanuma T., Focal plane instrumentation: a very high resolution MWPC system for inclined tracks. *Nucl. Instr. and Meth.* **141**, 459, 1977.

79. Sjoreen T. P., Ford J. L. C. Jr, Blankenship J. L., Auble R. L., Bertrand F. E., Gross E. E., Hensley D. C., and D. Schull, The vertical drift chamber as a high resolution focal plane detector for heavy ions, *Nucl. Instr. and Meth.* **224**, 421, 1984.

80. Charpak G., Sauli F., and Duinker W., High-accuracy drift chambers and their use in strong magnetic fields, *Nucl. Instr. and Meth.* **108**, 413, 1973.

81. Schroeder L. S., Streamer chambers- their use for nuclear science experiments, *Nucl. Instr. and Meth.* **162**, 395, 1979.

82. Bibber K. v. and Sandoval A., Streamer chambers for heavy ions, *Treatise on heavy ion science, vol 7,* Plenum press, New York, 1985.

83. Alard J. P., Arnold J., Augerat J., Babinet R., Bastid N., Brochard F., Costilhes J. P., Crouau M., De Marco N., Drouet M., Dupieux P., Fanet H., Fodor Z., Fraysse L., Girard J., Gorodetzky P., Gosset J., Laspalles C., Lemaire M. C., L'Hôte D., Lucas B., Montarou G., Papineau A., Parizet M. J., Poitou J., Racca C., Schimmerling W., Tamain J. C., Terrien Y., Valiro J., and Valette, The Diogene 4π detector at Saturne *Nucl. Instr. and Meth.* **261**, 379, 1987.

84. Mes H., Anderson H. L., Azuelos G., Blecher M., Bryman D. A., Burnham R. A., Carter A. L., Depommier P., Dixit M. S., Gotow K., Hargrove C. K., Hasinoff M., Kessler D., Leitch M., Macdonnald J. A., Mckee R. J., Martin J. P., Navon I., Numao T., Poutissou J. M., Poutissou R., Schlatter P., Spuller J., and Wright C. S., Update on the TPC at TRIUMF, *Nucl. Instr. and Meth.* **225**, 547, 1984.

85. Rai G., Arthur A., Bieser F., Harnden C. W., Jones R., Kleinfelder S., Lee K., Matis H. S., Nakamura M., McParland C., Nesbitt D., Odyniec G., Olson D., Pugh H. G., Ritter H. G., Symons T. J. M., Wieman H., Wright M., Wright R., and Rudge R., A TPC detector for the study of high multiplicity heavy ion collisions, *IEEE trans. on nucl. sci.* **37**, 56, 1990.

86. Beyerle G., Glatz A., Gnirs M., Herrmann N., Jackel W., Linke R., Pelte D., Schlesier R., Trzaska M., and Winkler U., The central drift chamber of the 4π detector, *GSI scientific report 1990,* Darmstadt, 1991.

87. Daues H. W., Fodor Z., Gaiser H., Gobbi A., Grösch H., Reindl M., Stelzer H., Ero J., Kecskemeti J., Koncz P., and Seres Z., Status of the HELITRON of the 4π detector, *GSI scientific report 1990,* Darmstadt, 1991.

88. Bagge E. and Christiansen J., The parallel plate counter as a self quenching particle measuring equipment, Naturwissenschaften **39**, 298, 1952.

89. Breskin A., Progress in low-pressure gaseous detectors, *Nucl. Instr. and Meth.* **196**, 11, 1982.

90. Sernicki J., Timing properties of transmission avalanche counters at moderate specific ionization, *Nucl. Instr. and Meth.* **A251**, 81, 1986.

91. Stelzer H., A large area parallel plate avalanche counter, *Nucl. Instr. and Meth.* **133**, 409, 1976.

92. Breskin A. and Zwang N., A fast bidimensional position sensitive parallel plate avalanche counter (PPAC) for light and heavy particles, *IEEE Trans. Nucl. Sci.*, **25**, 126, 1978.

93. Gaiardo D., Lelong P., Roussel P., and Volkov P., private communication.

94. Gaiardo D., Lelong P., and Volkov P., Delay lines in heavy ion detectors, IPNO-84-05, Orsay, 1984.

95. Hempel G., Hopkins F, and Schtz G., Development of parallel plate avalanche counters for the detection of fission fragments, *Nucl. Instr. and Meth.* **131**, 445, 1975.

96. Harrach D. v. and Specht H. J., A square meter position sensitive parallel plate detector for heavy ions, *Nucl. Instr. and Meth.* **164**, 477, 1979.

97. Kusterer K., Betz J., Harney H. L., Heck B., Liu Ken Pao, and Porto F., A gas detector system for mass and charge identification of heavy ions, *Nucl. Instr. and Meth.* **177**, 485, 1980.

98. Butler P. A., Connel K. A., Burrows J. D., El-Lawindy A. M. Y., Guidry M. W., James A. N., Jones G. D., Lauterbach C., Morrison T. P., and Simpson J., The application of a multiple gas counter spectrometer to the study of heavy ion reactions, *Nucl. Instr. and Meth.* **A239**, 221, 1985.

99. Orr N. A., Mittig W., Fifield L. K., Lewitowicz M., Plagnol E., Schutz Y., Zhan Wen Long, Bianchi L., Gillibert A., Belezyorov A. V., Lukyanov S. M., Penionzhkevich Y. E., Villari A. C. C.,

Cunsolo A., Foti A., Audi G., Stéphan C., and Tassan-Got L., New mass measurements of neutron rich nuclei near N = 20, *Phys. Lett.* **B258**, 29, 1991.

100. Breskin A., A subnanosecond low pressure MWPC for heavily ionizing particles, *Nucl. Instr. and Meth.* **141**, 505, 1977.

101. Binon F., Bobyr V. V., Duteil P., Gouanere M., Hugon L., Spighel M., and Stroot J. P., Low pressure multiwire proportional chambers with high time resolution for strongly ionizing particles, *Nucl. Instr. and Meth.* **94**, 27, 1971.

102. Breskin A., Chechik R., and Zwang N., Heavy ion timing with very low pressure MWPCs, *Nucl. Instr. and Meth.* **165**, 125, 1979.

103. Golovatyuk V. M., Ivanov A. B., Nikitin V. A., Peshekhonov V. D., and Zanevsky Yu. V., A low pressure proportional chamber with a high space resolution,*Nucl. Instr. and Meth.* **145**, 437, 1977.

104. Charpak G., Will gaseous detectors become routine tools in biology and medicine? *Nucl. Instr. and Meth.* **A283**, 371, 1989.

105. Stelzer H., Multiwire chambers with a two-stage gas amplification, *Nucl. Instr. and Meth.* **A310**, 103, 1991.

106. Izycki M., Martin M., Rosselet L., and Solomey N., A large multistep avalanche chamber: description and performance, *Nucl. Instr. and Meth.* **A310**, 98, 1991.

107. Breskin A., Chechik R., Fraenkel Z., Jacobs P., Tserruya I., and Zwang N., Low pressure multistep detector for very low energy heavy ions, *Nucl. Instr. and Meth.* **221**, 363, 1984.

108. Angelini F., Bellazini R., Brez A., Massai M. M., Spandre G., Torquati M. R., Bouclier R., Gaudens J., and Sauli F., The microstrip gas chamber, *Nucl. Phys.* **23A**, 254, 1991.

109. Oed A., Position sensitive detector with microstrip anode for electron multiplication with gases, *Nucl. Instr. Meth.* **A263**, 351, 1988.

110. Bouclier R., Florent J. J., Gaudaen J., Millon G., Pasta A., Ropelewski L., Sauli F., and Shekhtman L. I., High flux operation of microstrip gas chambers on glass and plastic supports, *Nucl. Instr. Meth.* **A323**, 240, 1992.

111. Barasch E. F., Bowcock T. J. V., Demroff H. P., Elliot S. M., Howe M. R., Lee B., Mazumdar T. K., McIntyre P. M., Pang Y., Smith D. D., Wahl J., Wu Y., Yue W. K., Gaedke R. M., and Vanstraelen G., Gas microstrip chambers, *Nucl. Instr. Meth.* **A315**, 170, 1992.

112. Angelini F., Bellazini R., Brez A., Decarolis G., Magazzu C., Massai M. M., Spandre G., and Torquati M. R., Results from the first use of microstrip gas chambers in a high energy physics experiment, *Nucl. Instr. Meth.* **A315**, 21, 1992.

113. Angelini F., Bellazini R., Bosisio L., Brez A., Massai M. M., Spandre G., and Torquati M. R., A microstrip gas chamber on a silicon substrate, *Nucl. Instr. Meth.* **A314**, 450, 1992.

114. Biagi S. F., Jackson J. N., Jones T. J., and Taylor S., Initial investigations of the performance of a microstrip gas avalanche chamber fabricated on a thin silicon dioxide substrate, *Nucl. Instr. Meth.* **A323**, 258, 1992.

115. Nagae T., Tanimori T., Kobayashi T., and Miyagi T., Development of microstrip gas chambers with multi-chip technology, *Nucl. Instr. Meth.* **A323**, 236, 1992.

116. Oed A., Geltenbort P., and Budtz-Jørgensen C., Substratum and layout parameters for microstrip anodes in gas detectors, *Nucl. Instr. Meth.* **A310**, 95, 1991.

117. Budtz-Jørgensen C., Bahnsen A., Olesen C., Madsen M. M., Jonasson P., Schnopper H. W., and Oed A., microstrip proportional counters for X-ray astronomy, *Nucl. Instr. Meth.* **A310**, 82, 1991.

118. Hartjes F., Hendriksen B., Schmitz J., Schijlenburg H., and Udo F., Operation of the microstrip gas detector, *Nucl. Instr. Meth.* **A310**, 88, 1991.

119. Angelini F., Bellazini R., Brez A., Massai M. M., Spandre G., and Torquati M. R., A microstrip gas avalanche chamber with two-dimensional readout, *Nucl. Instr. Meth.* **A283**, 755, 1989.

120. Barbosa A. F., Riekel C., and Wattecamps P., Two-dimentional X-ray detector based on microstrip and multiwire design, *Nucl. Instr. Meth.* **A323**, 247, 1992.

121. Angelini F., Bellazini R., Bosisio L., Brez A., Massai M. M., Perret A., Spandre G., and Torquati M. R., A microstrip gas chamber with true two-dimensional and pixel readout, *Nucl. Instr. Meth.* **A323**, 229, 1992.

122. Richter J., Large size microstrip particle detectors, *Nucl. Instr. Meth.* **A323**, 263, 1992.

123. Proceeding of the Sixth International wire chamber conference, Vienna, 1992. *Nucl. Instr. Meth.* **A323**, 1992.